Probabilistic statistical and agent-based encounter-impact models for fish and tidal turbine interactions

Jezella Ileana Peraza

A thesis

submitted in partial fulfillment of the

requirements for the degree of

Master of Science

University of Washington

2024

Committee:

John K. Horne

Andrew M. Berdahl

Andrea E. Copping

Samuel S. Urmy

Program Authorized to Offer Degree:

College of the Environment

Aquatic and Fishery Sciences

University of Washington

Abstract

Probabilistic statistical and agent-based encounter-impact models for fish and tidal turbine interactions

Jezella Ileana Peraza

Chair of the Supervisory Committee:

John K. Horne

School of Aquatic and Fishery Science

Marine Renewable Energy has potential to become a valuable and predictable energy source in regions with strong tidal and ocean currents. Tidal energy is a prominent sector within the industry but concerns regarding its potential impact on marine life hinder its development and deployment. Concerns include animal-turbine encounters, collisions with turbine structures, blade strikes, and risk of injury or mortality. Statistical and simulation models are employed to assess encounter and interaction risks between aquatic animals and tidal turbines, yet there is a need for a comprehensive model incorporating animal trajectories and behaviors. This study aims to develop an encounter-impact probability model, using acoustic and hydrodynamic data from Admiralty Inlet, Washington, USA, and insights from published literature.

Our encounter-impact model calculates conditional probabilities of fish-turbine interactions in sequential steps by incorporating empirical data and considering factors such as avoidance behavior and turbine dimensions. The model evaluates collision and blade strike risks, employing published values and empirical measurements, to assess overall impact probabilities.

The statistical, encounter-impact model assesses probabilities of fish-turbine interactions influenced by turbine type, time of day, and avoidance behavior. As an agent-based simulation, the probability model assesses fish-turbine interactions considering factors of animal behaviors and tidal flow. Fish locomotion and aggregation behaviors are simulated, incorporating active and passive avoidance of turbines. Interactions between fish and turbines (i.e., collision and/or blade strike) are simulated. Experimental factors like fish abundance, aggregation, and tidal speeds are explored to understand their effect on fish avoidance and potential interactions. Lastly, results from the statistical and agent-based model are compared.

For the statistical model, probabilities of fish presence vary between turbine type and avoidance scenarios, with collision, blade strike, and combined impact probabilities spanning several orders of magnitude. Light cycles slightly influence probabilities, with higher estimates observed at night. Turbine size also influences interaction probabilities, with larger turbines posing higher risks. Results from the agent-based model found that probabilities depend on aggregation behavior and tidal speed for both axial and cross-flow turbines. As expected, zone of influence and entrainment probabilities decrease with increasing tidal flow, while asocial fish are unaffected by changes in current speed. Overall impact probabilities increase with tidal speed for both turbine types and are primarily observed when fish are within social groups. Comparison between the simulation and statistical model reveals differences in mean probabilities for each model component. While both models rely on empirical data and literature values, there remain knowledge gaps in estimating potential impacts and turbine avoidance. Future research should focus on validating encounter-impact models with real-world data to enhance mitigation efforts and conservation strategies.

Table of Contents

List of Figures

List of Tables

Acknowledgments

First, thank you to my faculty advisor, John Horne, for guiding me through my thesis work and my time as a graduate student. I am grateful for the dedication and support you have shown towards my research, as well as your mentorship in fostering my development as a scientist.

Many thanks to my committee for providing me support and guidance; especially Andrew Berdahl for his valuable insights on agent-based modeling and for addressing all my queries, Andrea Copping for sharing her expertise in the marine renewable industry and for connecting me with professionals in the field, and Sam Urmy for his mentorship in navigating graduate school and for his assistance with coding and project strategy.

I am appreciative for the moral support of the members of the Fisheries Acoustic Research and Complex Ecological Systems Labs. Special thanks to Brendan Wallace, who was so generous to dedicate time and energy in developing the agent-based simulation model and providing clear explanations related to Python.

Muchisimas gracias to my beautiful family, for being my primary source of love, laughter, and encouragement. It is because of your patience and support who have shaped me into the woman I am today.

This research was funded by a Department of Energy grant (DE-EE-0006816.0000) to the ALFA project with additional financial support of Graduate Fellowships from the School of Aquatic and Fishery Sciences. Many thanks to the Clairmont L. and Evelyn S. Egtvedt Fellowship Fund in Fishery Sciences, the Martin Hall Fellowship for Fishery Innovations in Sustainability, the Kiyoshi G. Fukano Memorial Endowment, and the H. Mason Keeler Endowment for Excellence.

Dedication

A mis abuelos:

Gracias por siempre ser mi angel guardian.

Chapter 1. Introduction

1.1 General Introduction

In regions characterized by tidal and ocean currents, Marine Renewable Energy (MRE) could potentially play an important role in energy supply and climate change mitigation (Pelc & Fujita, 2002). MRE offers a consistent energy source with reduced carbon emissions, rendering it more predictable compared to other renewable sources such as wind or solar power (Zhang et al., 2017). Within the diverse realm of the MRE industry, tidal energy is one prominent sector that can harness power from tidal flows. However, development and deployment of tidal turbines remains in its early stages, largely influenced by apprehensions regarding their potential impact on marine life (Copping & Hemery, 2020). Primary concerns include potential animal-turbine encounters (e.g., Wilson et al., 2006), collisions with stationary turbine structures (Müller et al., 2023), blade strikes by rotating turbine blades (e.g., Castro-Santos & Haro, 2015; Courtney et al., 2022), and the consequential risk of injury or mortality (Copping et al., 2023; Hemery et al., 2021). Given the uncertainties surrounding these potential impacts, there is a need to comprehend physical and biological factors influencing potential interactions between aquatic animals and tidal turbines.

Quantifying probabilities of encounters and interactions between animals and tidal turbines will help resolve the perceived risk in the operation of tidal devices in the United States (Copping et al., 2020a). Currently, standard monitoring efforts to observe, characterize, and quantify encounter-impact risks are lacking, which impedes permitting and consenting of tidal turbines throughout the world. Developers are required by regulators to perform sustained monitoring to enhance mitigation measures (Rose et al., 2023; Schmitt et al., 2017), but it is not easy to collect data in dynamic sites (e.g., Williamson et al., 2017). The limited ability to obtain ecological data at tidal sites is directly attributable to sites being high energy environments (Shields et al., 2011)

with peak tidal flows routinely exceeding 2.5 ms^{-1} (e.g., Bevelhimer et al., 2017; Horne et al., 2013; Sanderson et al., 2023). Ecological data constraints can lead to poorly designed studies or few survey efforts which pose a lower likelihood of detecting impacts (Maclean et al., 2014), hindering progress of development (Copping & Hemery, 2020). Identifying knowledge gaps can provide guidance to needed observations and monitoring efforts to obtain empirical data required to characterize and assess potential interactions.

Potential impacts of tidal devices on aquatic animals can be assessed at individual and population scales. Numerous methodologies are employed to quantify risks associated with animal-turbine encounters and interactions. Approaches include statistical (Band et al., 2016; Bangley et al., 2022; Sanderson et al., 2023; Shen et al., 2016; Wilson et al., 2006) and simulation (Goodwin et al., 2014; Grippo et al., 2020; Romero-Gomez & Richmond, 2014; Rossington & Benson, 2020) modeling, empirical data collection (Bangley et al., 2022; Courtney et al., 2022; Polagye et al., 2020; Sanderson et al., 2023; Viehman et al., 2015; Viehman & Zydlewski, 2015; Williamson et al., 2016, 2017), and controlled laboratory studies (Berry et al., 2019; Copping et al., 2017; Müller et al., 2023; Onoufriou et al., 2019; Yoshida et al., 2020, 2021; Zhang et al., 2017). Among these approaches, most research has focused on using statistical and simulation modeling for animal-turbine interaction assessments (Roche et al., 2016).

There are two categories of models that can be used to estimate individual and population encounter and interaction risk: statistical and simulation modeling. Most statistical encounter-impact models have adopted modeling frameworks of the Encounter Rate Model (ERM) (Wilson et al., 2006) or the Collision Risk Model (CRM) (Band, 2012; Band et al., 2016) to estimate interactions between animals and turbines. The ERM is derived from a predator-prey model that integrates the volume occupied by the predator, size and density of prey, and swimming velocities

of both predators and prey. An encounter is defined when an animal and turbine blade might interact without behavioral avoidance or the presence of hydrodynamic forces, allowing the animal to escape the device (Wilson et al., 2006). Assumptions within the ERM include vertical movement and swimming speed distributions of focal species, such as random direction and orientation relative to the water and device (Grant et al., 2014). Notably, this model does not account for avoidance behavior or preferred swimming directions through a tidal channel. CRM components include animal transit time, area of the tidal turbine rotor, and animal size. Animals in this model are assumed to be swimming toward the turbine rotor and exhibit no avoidance behavior. Unlike the ERM where species are assumed to approach the device randomly, the CRM assumes if an animal is diving or parallel to the three-bladed turbine rotor an interaction will not occur (Grant et al., 2014). Both the ERM and CRM share a commonality in that they lack behavioral components accounting for active and passive avoidance. To address some of these model limitations, modified ERM and CRM models incorporate elements such as avoidance and depth distributions (Joy et al., 2018), injury risk from turbine blades (Copping & Grear, 2018), and a coupled agent-based model to simulate behavior (Rossington & Benson, 2020).

Numerous statistical models designed for individual animal and turbine assessments are developed from empirical data collected from tidal energy project sites to quantify potential encounters and impacts. Shen *et al.* (2016) presented empirical evidence of fish actively avoiding an MRE device as far away as 140 meters. The resulting encounter model incorporated probabilities related to fish being at device-depth, the likelihood of fish altering behavior to avoid the device, and the probability of fish behavioral changes occurring during their approach to the device (Shen et al., 2016). Using acoustic telemetry data, Bangley *et al.* (2022) tracked fish across diverse hydrodynamic conditions at a tidal site, and incorporated these data into an encounter rate

model. Their approach assessed the probability of striped bass (*Morone saxatilis*) presence, contingent on hydrodynamic conditions. Similarly, Sanderson *et al.* (2023) used acoustic telemetry to quantitatively assess probabilities of Atlantic salmon (*Salmo salar*) encounters within a turbine installation. Additionally, their research delved into measuring detection efficiency of acoustic tag signals under highly turbulent tidal conditions (Sanderson et al., 2023), strengthening accuracy of encounter probability estimates. Copping *et al.'s* (2023) study proposes a conceptual framework for assessing animal-turbine collision risk using a probabilistic approach to analyze animal proximity and potential turbine blade impacts. The authors used data from Bangley *et al.* (2022) to showcase their model's applicability, specifically focusing on striped bass presence near a functioning turbine. This analysis encompasses the first three stages of their probabilistic framework.

On a population scale, Hammar *et al.'s* (2015) conceptual population collision risk model quantified a fish population encountering an array of tidal turbines assuming behavioral avoidance. Despite there not being empirical data to validate the model, Hammar *et al.* (2015) applied avoidance behaviors (i.e., avoidance failure, evasion failure) and other turbine-specific stressors (i.e., hydraulic stress, Cada et al., 2007). A lack of empirical data led Hammar *et al.* (2015) to include avoidance behavior information from a previous freshwater video surveillance experiment (Hammar et al., 2013) for variable parameterization. The Exposure Time Population Model (ETPM) (Grant et al., 2014) estimates collision (i.e., animal-turbine blade interaction) rates necessary to achieve a mortality rate for diving birds. Likely exposure to risk is calculated in the ETPM using the number of animals in a population and the amount of time an animal spends within a tidal site (Grant et al., 2014). While currently tailored for diving birds, there is potential to adapt the model to other marine animals given sufficient data. The diverse array of individual

and population statistical models aimed at quantifying animal-turbine interactions introduces parameterized components that can be tailored to specific species and site characteristics, contributing to refined estimations of associated risks.

Simulation modeling is another approach to characterize individual and population interactions with an MRE device. These models can integrate external environmental conditions and individual behavioral characteristics, which can support current knowledge gaps surrounding animal avoidance and behavior at tidal sites. Goodwin *et al.* (2014) uses the Eulerian-Lagrangian-Agent Method (ELAM) to simulate three-dimensional movement patterns of individual fish responding to abiotic stimuli in a hydropower dam environment. This model encompasses Eulerian components to describe hydrodynamics, Lagrangian components to simulate movement trajectories of individuals, and agent components detailing individual behavior decisions (Goodwin et al., 2012). To model fish movement through rivers where manufactured obstacles are present, Goodwin *et al.* (2014) uses ELAM to model the flow field at a dam site along with fish swimming speed and orientation. Similarly, Grippo *et al.* (2020) uses ELAM to combine a local hydrodynamic model of Cobscook Bay, Maine with data from mobile hydroacoustic fish surveys described in Shen *et al.* (2016) to simulate potential encounters in a flow field around an MRE device. ELAM applied in Grippo *et al.* (2020) combines hydroacoustic fish distributions with hydrodynamic modeling simulations to quantify fish behavioral responses in a tidal turbine flow field before, during, and after encountering a device.

While ELAM can model fish behavior in proximity to a tidal device, it lacks specific insights into direct interactions with turbine components. In contrast, Romero-Gomez & Richmond (2014) developed a blade strike and fish survival rate model, using computational fluid dynamics with Lagrangian particle tracking in a simulated turbulent environment. Their model quantifies

axial-flow turbine blade strikes on fish based on turbulence, fish size and distribution, flow velocity, and turbine rotational speed (Romero-Gomez & Richmond, 2014). Despite including potential blade strikes, behavioral responses of fish avoiding turbine blades were not included in the model. Additionally, Rossington & Benson (2020) couple Band *et al.'s* (2016) CRM with an agent-based simulation. Model integration considers hydrodynamic conditions, behavioral traits, and active locomotion to estimate interaction rates previously obtained in Band *et al.* (2016). While this model doesn't explicitly include avoidance, it incorporates crucial behavioral traits such as vertical migration, probability of navigation, response to external stimuli, and agent decision-making. Simulation modeling serves as a valuable tool for providing insights into hydrodynamics and animal characteristics that may not be explicitly included in statistical models. Incorporating additional parameters such as behavioral traits can refine probability estimates of encounter and impact and provide empirical guidance on avoidance behaviors. Notably, recognizing that outcomes of simulation models are contingent upon model assumptions and behavioral rules associated with existing data and biological and physical reasoning.

After review, there lacks a comprehensive statistical and simulation-based model that details animal trajectories, behaviors, and potential interactions as fish approach and encounter a tidal turbine. Lack of sufficient empirical data regarding fish approaches, encounters, and direct interactions further complicates parameterization and validation of encounter-impact models. During the validation of these models, it is important to distinguish specific components impacted by this limitation to identify areas where additional behavioral attributes can be incorporated to enhance probability estimates.

1.2 Objectives

The goals of this study are to develop statistical and agent-based probability encounter-impact models that include parameters that have not been used in published models. The encounter-impact model will be parameterized using acoustic and hydrodynamic data from Admiralty Inlet, Puget Sound, Washington (Horne et al., 2013), as well as parameter values from published literature. Throughout this thesis, the goal is to answer the following questions: 1) How to formulate an encounter-impact probability model to quantify interactions between fish and tidal turbine devices? 2) How do probability estimates differ between the two modeling approaches? and 3) Can data and knowledge gaps be identified from results of the two models that can be used to guide future research and model applications?

Chapter 2. Using a statistical model to quantify conditional probabilities of fish and tidal turbine interactions

This chapter is a modified version of "Quantifying conditional probabilities of fish-turbine encounters and impacts" published in *Frontiers in Marine Science*.

2.1 Introduction

Tidal energy is at an early stage of development and deployment compared to on and offshore wind turbines, despite both technologies facing similar complications regarding potential effects on wildlife. Potential risks such as encounters, collisions with stationary turbine structures (Müller et al., 2023), strikes by rotating turbine blades (e.g., Castro-Santos & Haro, 2015; Courtney et al., 2022), and injury/mortality rates (Hemery et al., 2021) are perceived as threats to animal populations and can impede development of renewable energy sites. Adequate baseline and post-installation monitoring data are unavailable concerning potential environmental effects at sites, resulting in high degrees of uncertainty among regulators who take precaution in continuing efforts for full-scale MRE commercial development (Copping et al., 2020b).

Quantifying interaction rates between animals and tidal turbines remain a challenge due to limited field opportunities and appropriate monitoring technologies (Fox et al., 2018). Globally, operational acoustic and optical technologies deployed for monitoring tidal energy sites are scarce (Copping et al., 2021). One type of technology is hydroacoustics, providing noninvasive, continuous sampling of the entire water column in high-energy tidal environments (e.g., Shen et al., 2016; Viehman et al., 2015). Echosounders, both stationary and mobile, monitor biomass by transmitting sound pulses and analyzing their reflections to measure size, count, and potentially identify species. Acoustic cameras offer real-time visualization of potential interactions, particularly with larger animal targets (Bevelhimer et al., 2017; Staines et al., 2020, 2022). While

various technologies are available, their deployment is often restricted by operational constraints, including limited detection of weaker targets (Williamson et al., 2017) and challenges in sampling high-energy flowing environments. An additional approach involves the use of models to estimate the probability of animal-device interactions when empirical data on animal behavior and hydrodynamics are limited (Buenau et al., 2022).

To estimate fish and tidal turbine interactions, a model must quantify conditional probabilities of fish approaching and interacting with a turbine in sequential steps. Current models are limited by the lack of active and passive avoidance behavior of fish at varying distances from a turbine (c.f. Chapter 1). Therefore, a complete model should incorporate both types of behavior. Risks such as collisions with stationary, nonrotating components of the device are also lacking in published models (Müller et al., 2023; Peraza & Horne, 2023). These collisions could disorient fish (Courtney et al., 2022) and potentially lead to subsequent blade strikes. To understand these potential effects, information regarding avoidance and additional risk types incorporated into a conditional encounter-impact model must be presented to regulators to improve understanding of MRE technologies and development (Rose et al., 2023).

This study aims to develop a flexible, probabilistic statistical model that quantifies encounters and impacts between fish and tidal turbines. The model will include parameters not widely studied in existing literature, such as avoidance and collisions with stationary structures. Using acoustic data from Admiralty Inlet, WA, USA, and literature values, the encounter-impact model will estimate probabilities of encounter, collision, blade strike, and sequential collision and blade strike between fish and arbitrary tidal turbines. Identifying data gaps and determining appropriate next steps for model application will follow acquisition of model probabilities.

2.2 Methods

2.2.1 *Model description*

The encounter-impact model computes probabilities for individual model components, and conditional probabilities of fish approaching and potentially interacting with a tidal turbine in sequential steps (Figure 1).

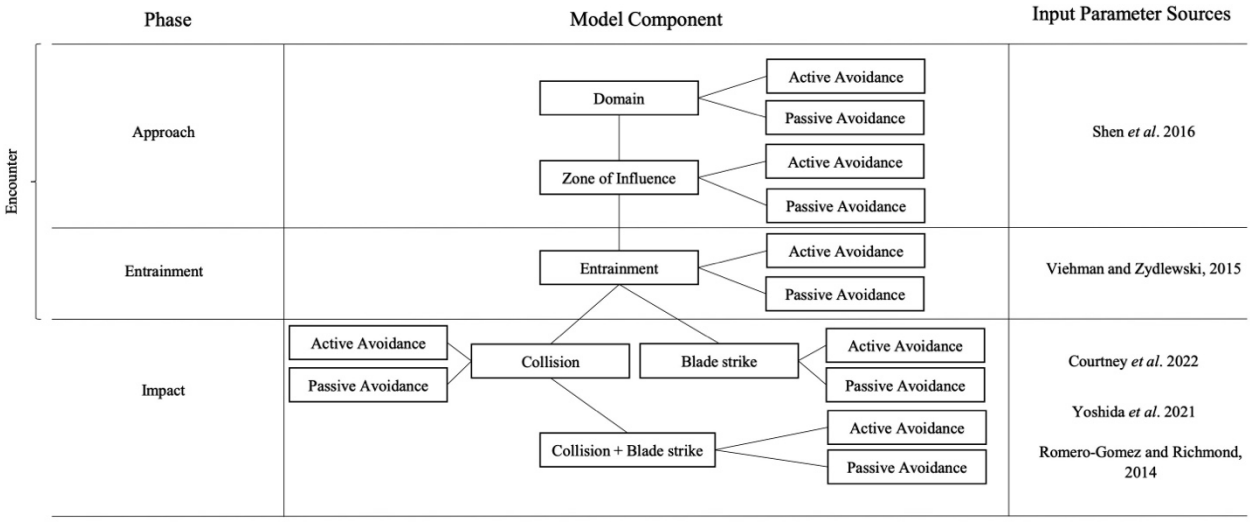

Figure 1. A schematic of the statistical encounter-impact probability model. The left column identifies the model phase, the center column details model components, and the right column identifies literature used to extract parameter values that are used in corresponding model components.

The approach phase quantifies when an animal enters the vicinity of an MRE device and includes the model domain, zone of influence, and estimates of active and passive avoidance. The model domain is defined as the study region encompassing the population of interest. If fish are present, then the domain model component is assigned a probability value of 1 (Table 1). We define the zone of influence as the region which an animal is capable of sensing and reacting to the turbine. Shen *et al.* (2016) used mobile hydroacoustics to track fish approaching a cross-flow

tidal turbine and observed responses to a turbine by fish, measured using change in swimming direction, at distances over a hundred meters (m). In this model, the zone of influence is set to this 140 m distance upstream from a tidal turbine (Figures 2A, B). A vertical height of 25 m above the seafloor is used to represent approximately twice the vertical footprint of a proposed turbine in Admiralty Inlet (Jacques, 2014) and is within Shen *et al.'s* (2016) range of water depths (25 m at low tide to 32 m at high tide) at their study site. The probability of being within the zone of influence is dependent on the device's shape and size, water depth, range of tidal current speeds, and fish swimming speed. The probability of being in the zone of influence is defined as the probability of a fish being within the domain multiplied by the complement of an individual avoiding the device (Table 1).

Table 1. Probability equations for each component of the encounter-impact model.

Model component	Probability equation
Domain	P(Domain) = [1, 0]
Zone of Influence	P(Zone of Influence) = 1 * P(1 – Avoid)
Entrainment	P(Entrainment) = P(Zone of Influence) * P(1 – Avoid | Zone of Influence)
Collision	P(Collision) = P(Entrainment) * P(Collision | Entrainment)
Blade strike	P(Blade strike) = P(Entrainment) * P(Blade strike | Entrainment)

Collision and Blade strike	P(Collision and Blade strike) = P(Entrainment) * [P(Collision) * P(Blade strike | Collision)]
Overall Impact	P(Overall Impact) = {1 * P(1 – Avoid) * [P(Zone of Influence) * P(1 – Avoid | Zone of Influence)] * [P(Entrainment) * P(Collision | Entrainment)]} + {1 * P(1 – Avoid) * [P(Zone of Influence) * P(1 – Avoid | Zone of Influence)] * [P(Entrainment) * P(Blade strike | Entrainment)]} + {1 * P(1 – Avoid) * [P(Zone of Influence) * P(1 – Avoid | Zone of Influence)] * [P(Entrainment) * (P(Collision) * P(Blade strike | Collision))]} *Simplified:* P(Overall Impact) = P(Collision) + P(Blade strike) + P(Collision and Blade strike)

Entrainment occurs when a fish is within the area adjacent to the device, normal to the device face. If an animal continues its current trajectory with no avoidance, it will collide with the turbine base or be struck by a turbine blade. The turbine base and entry area are half the vertical height of the turbine (Figures 2A, B). Areal dimensions of the cross-flow turbine base (i.e., vertical-axis turbines that rotate blades perpendicular to tidal flow direction) and turbine entrance are both 30 m by 10 m. Areal dimensions of the axial-flow turbine base (i.e., horizontal-axis turbines that rotate blades facing direction of flow) and turbine entrance are 5 m by 10 m. The probability of entrainment is defined as the probability of a fish being within the zone of influence multiplied by the probability of 1 minus avoiding the device given that the individual is within the zone of influence (Table 1).

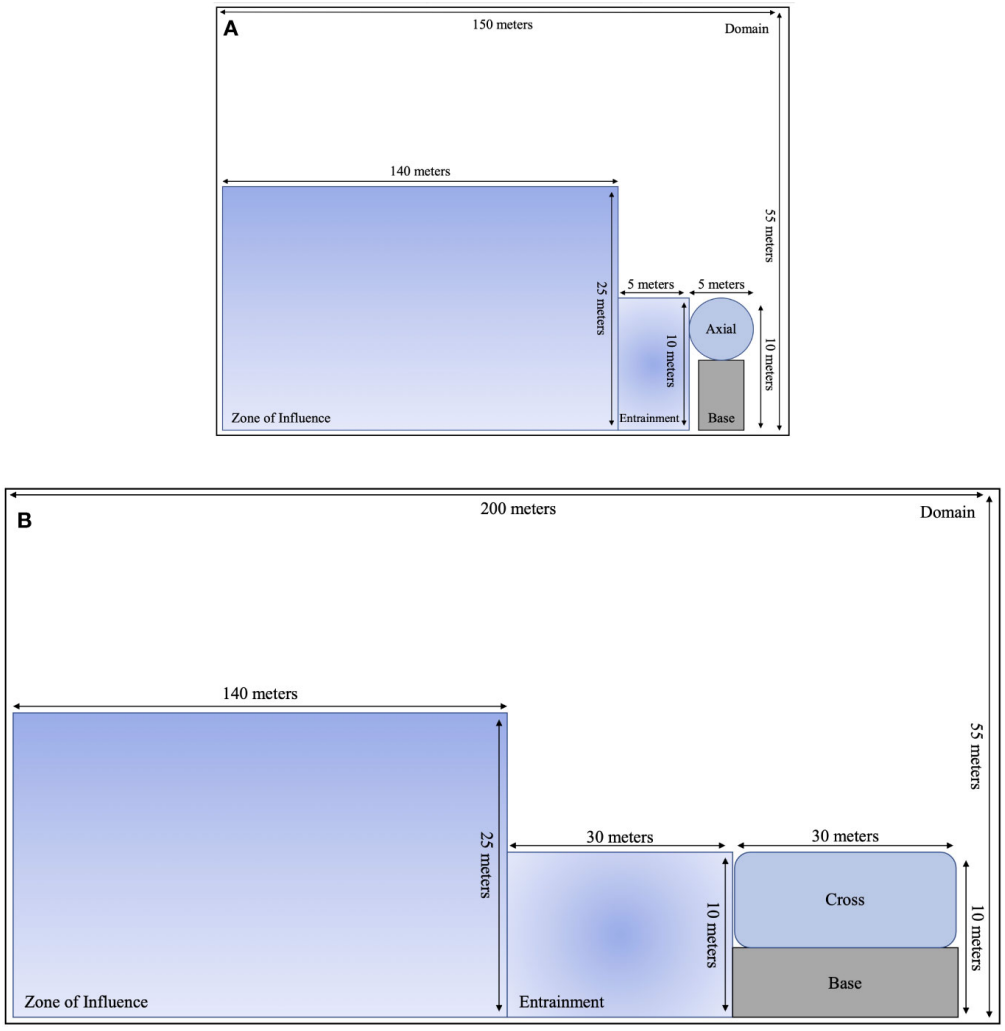

Figure 2. A two-dimensional schematic showing dimensions of the encounter-impact model components for (A) axial and (B) cross-flow turbines.

Interactions between a fish and a tidal turbine are composed of collisions and/or blade strikes. We define collision as physical contact between an animal and the turbine base or a non-moving device component (e.g., Müller et al., 2023). We define blade strike as contact between an animal and a rotating blade (e.g., Castro-Santos & Haro, 2015; Courtney et al., 2022). In the model, collision and blade strike are treated as potential sequential events, where fish can collide with a turbine support structure and then be struck by a rotating blade. This might be an untrivial interaction as turbine dimensions can exceed 15 to 20 m in length and width (c.f. Courtney et al.,

2022; Shen et al., 2016; Viehman & Zydlewski, 2015), which provides large surface areas for fish to collide with a turbine base or non-rotating structures when active avoidance is not possible.

Impact is defined as one or more interactions between a fish and a turbine through collision and/or blade strike. Blade strikes constitute the greatest risk to fish and are a concern among researchers and regulators (Copping et al., 2020b). Therefore, most experimental (Yoshida et al., 2020, 2021) and field (Courtney et al., 2022) research has been done to quantify blade strike rates. Impact probabilities are calculated for each model subcomponent and overall potential impact (Table 1) based on field (Courtney et al., 2022), laboratory (Yoshida et al., 2020, 2021), and simulation model (Romero-Gomez & Richmond, 2014) blade strike data. All impact probabilities depend on whether an animal is present within the entrainment area. The probability of collision with a turbine is calculated as the probability of entrainment multiplied by the probability of collision given that a fish is entrained. The probability of blade strike is defined as the probability of entrainment multiplied by the probability of a blade strike given that a fish has entered the device. Lastly, the probability of collision and blade strike is defined as the probability of entrainment, multiplied by the probability of collision, multiplied by the probability of blade strike given that a fish collided with the device. The overall probability of impact is calculated as the sum of the three potential interaction events: collision, blade strike, and collision and blade strike.

All phases of the encounter-impact model include active and passive avoidance (Figure 1). Avoidance is defined as a change in a fish's trajectory in response to tidal devices. In behavioral studies, fish have been shown to actively avoid predation and navigate around obstacles, even at long distances (e.g., Bender et al., 2023; Berry et al., 2019; Muirhead & Sprules, 2003; Müller et al., 2023; Utne, 1997; Zhang et al., 2017). Tidal flow speeds often surpass fish swimming capabilities (c.f. Okubo, 1987, He, 1993), potentially leading to passive transport through the water

and passage around or through MRE devices. Therefore, the definition of avoidance is expanded to a fish's response and movement away from a device and/or its avoidance due to hydrodynamic forces (Copping & Hemery, 2020). We define the threshold between active and passive avoidance using the ratio of swimming capability to tidal flow. Average Pacific herring (*Clupea pallasii*) fork length from Admiralty Inlet net samples is used to estimate swimming speed using Okubo's (1987) locomotion equation:

$$SS = 2.69 \cdot L^{0.86} \quad (2.1)$$

where *SS* is swimming speed (ms^{-1}), and *L* is fish length (m). Active locomotion is assumed when the ratio of swimming speed to tidal flow is greater than 1 body length per second (bls^{-1}) (He, 1993). Passive locomotion occurs when the tidal speed exceeds 1 bls^{-1}, in this study 0.155 ms^{-1}.

2.2.2 *Tidal turbine dimensions*

For this study, representative axial and cross-flow tidal turbine devices are used in calculations of encounter and impact probabilities. Tidal turbine dimensions used are based on an axial-flow Verdant Power Kinetic Hydropower System (KHPS) (Bevelhimer et al., 2017) (Figure 2A) and a cross-flow Ocean Renewable Power Company TidGen Power System (Shen et al., 2016) (Figure 2B). Verdant Power KHPS turbine characteristics include a three-bladed, single-rotor turbine. The height of the device is approximately 10 m, with a rotor-swept area of 5 m in diameter, defining an area of 5 m by 10 m. The TidGen device is 31.2 m long and 9.5 m high with foils (i.e., rotating blades) 6.7 - 9.5 m above the seafloor, defining an area of 30 m by 10 m.

2.2.3 *Empirical data description*

Data were collected for the potential deployment of two Open Hydro (https://www.emec.org.uk/about-us/our-tidal-clients/open-hydro/) turbines in northerly Admiralty

Inlet, Puget Sound, Washington, a proposed tidal energy site in the Snohomish Public Utility District (Horne et al., 2013). The proposed site is approximately 750 m off Admiralty Head at a depth of 55 m mean tide level. Data sources included a 120 kHz Simrad EK-60 echosounder on a mobile surface vessel an autonomous bottom-deployed 1MHz Nortek AWAC acoustic doppler current profiler (ADCP), and midwater trawls conducted by the vessel.

The mobile echosounder operated from May 2 to May 13 and June 3 to June 14, 2011, day and night, where collected data were from 324 parallel transects that were 0.7 to 1.5 km long and 0.5 km apart, extending northwest and southeast of the proposed turbine location (see Horne et al., 2013 for survey details). The ADCP was used concurrently with the mobile echosounder to obtain tide state (slack, moderate, or extreme; flood, ebb) and tidal velocity measurements. The ADCP was deployed May 9-10, 2011, and retrieved June 9-10, 2011, and sampled for 12 minutes every two hours, resulting in 10% coverage of the entire deployment time (Jacques, 2014).

A Marinovich midwater trawl, a 6 m x 6 m box trawl fished with 4.6 m x 6.5 m steel V-doors, was used to capture samples to quantify species composition and length-frequencies of the fish community. Among captured species, Pacific herring was the most abundant species, comprising 32% of the total catch by number. Therefore, in this study, all acoustic backscatter is attributed to Pacific herring in acoustic density calculations. The average length of Pacific herring caught in the midwater trawl was 0.155 m and is used in all acoustic and swimming speed calculations. Given analogous fish lengths and time of year, the target strength conversion equation for Pacific herring from Thomas *et al.* (2002): $26.2 \cdot \log_{10}(L_{cm}) - 72.5$ is used to transform acoustic-derived densities ($m^2\ m^{-3}$) to fish densities (fish m^{-2}).

2.2.4 *Factors contributing to model component probabilities*

No turbine was deployed during data collection. Instead, the Admiralty Inlet dataset is used to explore possible impacts of multiple turbine types on different fish densities and distributions under different light regimes. To observe how acoustic densities varied with light, probabilities of fish presence for each model component during day and night are calculated for each turbine type. Fish densities are estimated by dividing each surveyed transect in horizontal 140 m, 30 m, or 5 m bins (corresponding to turbine type, Figures 2A, B) and then grouping bins to match the size of each model component.

Probability estimates in the encounter-impact model are also influenced by active and passive avoidance. The model uses three avoidance scenarios. The first scenario assumes fish are unable to avoid the turbine. In the second scenario, fish can avoid the turbine using active and passive avoidance. Active avoidance rates are estimated from the Admiralty Inlet dataset by multiplying the proportion (i.e., 0.372, Shen et al., 2016) of fish who avoid model components and the turbine. Passive avoidance rates are estimated by tabulating fish observations swimming around or above model components, assuming avoidance will occur to the side or above a device. The proportion of time passive avoidance occurs is determined by the tidal cycle – when tidal flow speeds surpass fish swimming speeds. The third scenario uses Shen *et al.'s* (2016) active avoidance rate of 0.372 without incorporating passive avoidance. When an avoidance rate from Admiralty Inlet or Shen *et al.* (2016) is incorporated into the model, estimates of fish impact are calculated using conditional probabilities from sequential model components. This approach evaluates a fish's ability to avoid a device across model components and provides insight into the likelihood of impact for each model phase and overall encounters with tidal turbines. When an avoidance rate

is not included, calculated impact probabilities are not dependent on sequential model components and analogous to rates in published studies.

2.2.5 *Estimating statistical probabilities*

Probabilities of fish presence during day and night is determined by enumerating acoustic abundance estimates detected within bins along each mobile survey transect, aligned with areas of each model component (Figures 2A, B). To obtain fish presence probabilities, acoustic density was derived in Echoview 12 (https://echoview.com) based on the factors and avoidance scenarios described. Acoustic energy was extracted by setting cell grids of 140 m by 25 m for the zone of influence, and 30 m by 10 m or 5 m by 10 m for the entrainment area along each transect. This energy, known as the area backscattering coefficient (Simmonds & MacLennan, 2005), can be converted to obtain density estimates of Pacific herring. Density of Pacific herring is calculated as the product of the area backscattering coefficient and model component areas divided by the backscattering cross-section (Simmonds & MacLennan, 2005). The backscattering cross-section is 7.39×10^{-5} m^2 in its linear form, obtained from the target strength equation $26.2 \cdot \log_{10}(L_{cm}) - 72.5$ (Thomas et al., 2002) using the average Pacific herring length of 0.155 m (Horne et al., 2013). Fish abundances in cells are summed to estimate total abundance for each transect. Probabilities of individual fish presence within each model component are determined by dividing the number of individuals detected within each cell of each model component by total fish abundance.

Since no data on fish-turbine interactions are available from Admiralty Inlet, encounter and impact published values are used in model calculations. At this time, there are no published probability estimates of collisions between fish and stationary tidal structures or collisions followed by blade strikes. Collision probabilities are estimated by calculating the complement of published blade strike probabilities and discounting by length-dependent swimming speed and

time of day avoidance rates published in Viehman & Zydlewski (2015). Blade strike probabilities are taken from field measurements (Courtney et al., 2022), laboratory experiments (Yoshida et al., 2021), and calculated using a blade-strike model (Romero-Gomez & Richmond, 2014):

$$P(strike) = \frac{nNL\cos(\alpha)}{U} \quad (2.2)$$

where *P(strike)* is the probability of a blade strike, *n* is the number of blades, *N* is a fixed rotation rate [i.e., 0.357 s^{-1} for a cross-flow turbine (Viehman & Zydlewski, 2015) and 0.667 s^{-1} for an axial-flow turbine (Bevelhimer et al., 2017)], *L* is fish length (m), α represents the fish approach angle perpendicular to the blade plane (α = 0), and *U* is tidal velocity (ms^{-1}). Blade strike probabilities are estimated using equation (2.2) for tidal velocities observed in Admiralty Inlet that ranged from 1.0 ms^{-1} to 3.0 ms^{-1} (Horne et al., 2013) in increments of 0.2 ms^{-1}. Incremental changes in tidal velocities depict the progression of a tidal cycle, yielding a range of strike probabilities in response to periodic flow conditions. The encounter-impact model also uses blade strike rates from Courtney *et al.* (2022) (0.13) and Yoshida *et al.* (2021) (0.02 – 0.05) in blade strike calculations. Inclusion of these rates in the blade strike model component compensates for limited data availability and introduces a range of probability estimates that incorporate turbine design, time of day, and turbine avoidance.

The sequential probability of collision and blade strike is determined by multiplying collision and published blade strike probability estimates. Probabilities of collision, blade strike, and collision and blade strike are reduced by avoidance rates in model calculations. Overall impact probabilities are calculated by summing estimated probabilities of each impact subcomponent (Table 1).

2.3 Results

Probabilities for each component of the encounter-impact model are influenced by turbine type, time of day, and avoidance. Based on their vertical distribution in Admiralty Inlet, approximately 6.36 to 6.49% of Pacific herring (hereafter fish) would be swept into zone of influence (Appendix A2.1, A2.2, A2.3, A2.4). If fish are within the zone of influence, 0.245 to 4.08% of those individuals are likely to be entrained with the device for an axial-flow turbine (Appendix A2.1, A2.2) and 1.18 to 4.08% of individuals for a cross-flow turbine (Appendix A2.3, A2.4). If entrained, probabilities of impact depend on events of collision, blade strike, or sequential collision and blade strike. About 0.0364 to 32.4% of fish that are entrained with the device will collide with both turbine types, and approximately 0.0261 to 40% of fish will be struck by the turbine's blades (Appendix A2.1, A2.2, A2.3, A2.4). If both events occur, about 0.000242 to 6.78% of fish might collide then be struck by either turbine type's blade (Appendix A2.1, A2.2, A2.3, A2.4). Overall, approximately 0.110 to 66.6% of fish will be impacted by an axial-flow turbine and 0.110 to 68.9% of fish will be impacted by a cross-flow turbine (Table 2).

Table 2. Impact probability estimates for axial and cross-flow turbines for avoidance scenarios using alternate blade strike probability estimates.

		Axial-Flow Turbine		Cross-Flow Turbine	
Avoidance scenario	Blade strike probability estimate	Day	Night	Day	Night
No avoidance	Courtney *et al.* 2022	0.172	0.455	0.172	0.455

	Yoshida *et al.* 2021	0.0928	0.353	0.0928	0.353
	Romero-Gomez and Richmond, 2014	0.436 - 0.175	0.666 - 0.171	0.337 - 0.138	0.689 - 0.423
Admiralty Inlet avoidance	Courtney *et al.* 2022	0.00204	0.00541	0.00204	0.00541
	Yoshida *et al.* 2021	0.00110	0.00419	0.00110	0.00419
	Romero-Gomez and Richmond, 2014	0.00515 - 0.00206	0.00805 - 0.00545	0.00907 - 0.00191	0.0176 - 0.00529
Shen *et al.* (2016) avoidance	Courtney *et al.* 2022	0.00687	0.0185	0.00687	0.0185
	Yoshida *et al*. 2021	0.00370	0.0144	0.00370	0.0143
	Romero-Gomez and Richmond, 2014	0.0164 - 0.00699	0.0276 - 0.0187	0.0304 - 0.00647	0.0357 - 0.0181

When comparing probabilities, about 0.194 to 10% fish are likely to interact with model components and the turbine at night than during the day for both turbine types (Appendix A2.1, A2.2, A2.3, A2.4). However, blade strikes are more likely to occur during day than at night, with an average 0.24% difference for the axial and cross-flow turbine (Appendix A2.1, A2.2, A2.3, A2.4). When comparing overall impact probabilities in light regimes, fish are more likely to interact with the device at night than during the day for both turbine types, with estimates ranging over three orders of magnitude (Table 2). Impact probabilities vary within three orders of magnitude depending on other parameters applied to the model. Turbine design influences impact probabilities, with an axial-flow turbine exhibiting the lowest risk of impact across factors and avoidance scenarios (Table 2).

As expected, fish are more likely to encounter each model component when no avoidance is included, where model components are not conditioned on preceding events in calculations (Appendix A2.1, A2.2, A2.3, A2.4). Probabilities are lowest when the proportion of fish in Admiralty Inlet were not in the vertical range of model components or turbine (see second avoidance scenario in 2.2.4), reflecting the inclusion of conditional probabilities in model calculations. The vertical distribution of fish within the zone of influence across all avoidance scenarios is the same for both turbine types (Appendix A2.1, A2.2, A2.3, A2.4). Fish are more likely to be entrained with the device when Shen *et al.'s* (2016) avoidance rate (4.08% of herring) is applied to the model for both turbine types (Appendix A2.2, A2.4). Probabilities of impact are highest by two to three orders of magnitude when no avoidance is included for a cross-flow turbine (Table 2). Collision probabilities (32.4% of herring), blade strike probabilities (40% of herring), and sequential collision and blade strike probabilities (6.78% of herring) are all highest for both turbine types when subcomponents are modeled with no avoidance (Appendix A2.1, A2.2, A2.3,

A2.4). Minimum and maximum probability values are similar between subcomponents and overall impact estimates, with larger values occurring when no avoidance is applied and lowest when avoidance rates from Admiralty Inlet are used in model calculations (Table 2).

Conditional probability estimates from this study are both lower and higher than other published values (Table 3). Shen *et al.* (2016) and Bangley *et al.* (2022) observed order of magnitude higher probabilities of fish approach and encounter with a tidal turbine than average approach estimates in this study. Similarly, Viehman & Zydlewski (2015) and Bevelhimer *et al.* (2017) found that approximately 18.8 and 15.4% of fish are directly aligned with a tidal device. Band *et al.* (2016) observed order of magnitude higher probabilities of collision for Harbor seals *(Phoca vitulina)* with turbine rotors when compared to results of this study. In contrast, Wilson *et al.'s* (2006) non-conditional encounter probabilities for Pacific herring are two orders of magnitude lower than those estimated in this study.

Regardless of the combination of factors, a minimum of 0.00242 to a maximum of 32.4% of fish will encounter or interact with a tidal turbine. Additionally, 0.110 to 68.9% of fish will potentially collide, be struck, or collide and then be struck by a tidal turbine. Probability values are particularly low when conditioned on fish occurring within a turbine's zone of influence, where subsequent entrainment may lead to an impact. All highest probability values occur at night with no avoidance in calculations for a cross-flow turbine.

Table 3. Comparison of average fish presence probabilities for each phase of the encounter-impact model to published literature values.

Encounter-Impact Model Phase	Encounter-Impact Model Probabilities		Literature Model Phase	Literature Results		Literature Source	Literature Focal Species
	Day	Night		Day	Night		
Approach	0.0636	0.0649		0.432		Shen *et al.* 2016	Unidentified
				0.15 – 0.4		Bangley *et al.* 2022	Striped bass
Entrainment	0.0200	0.0203		0.0432	0.333	Viehman and Zydlewski, 2015	Unidentified
	0.0200	0.0203		0.154		Bevelhimer *et al.* 2017	Unidentified
Collision	0.0126	0.0982	Collision	0.306		Band *et al.* 2016	Harbor seal
Blade strike	0.0567	0.0543	Encounter	0.000212		Wilson *et al.* 2006	Pacific herring
Collision and Blade strike	0.00243	0.0126	Encounter	0.000363		Wilson *et al*. 2006	Harbor porpoise

2.4 Discussion

Probabilities of fish presence within Admiralty Inlet and potential interaction with the tidal turbine are influenced by model component, time of day, turbine type, and avoidance scenario. Across all model components including overall impact, estimates of fish-turbine encounters and impacts are generally low, spanning one to four orders of magnitude. Impact probabilities are particularly low when conditioned on fish being within the zone of influence susceptible to entrainment by the device. Conditional events are crucial in understanding a fish's approach to a turbine situated hundreds of meters away and how fish can actively or passively avoid the device to prevent a potential interaction.

Influence of light and dark cycles on the vertical distribution of fish and impact probabilities is limited. Differences based on diel cycles are potentially driven by changes in herring vertical distribution (Munk et al., 1989), where a slight increase in probability values is observed for model estimates based on empirical data obtained at night compared to day. Studies in the field (Viehman et al., 2015; Viehman & Zydlewski, 2015; Williamson et al., 2019) and laboratory experiments (Yoshida et al., 2021) indicate that light intensity affects fish distribution in the presence of MRE devices. Williamson *et al.* (2019) noted a 2.63 times greater increase in fish aggregation rates around turbine structures at night compared to day, supporting previous findings that indicate higher probabilities of turbine entry for fish at night (Viehman & Zydlewski, 2015). Viehman *et al.* (2015) reported that fish are more evenly distributed at night, highlighting fish presence in dark conditions where turbines are present. Results from our study and current literature suggest that analyzing fish behavior in light and dark conditions can provide insights into fish-turbine detection distances and potential interactions.

Fish approaching and encountering tidal turbines at various distances are observed in controlled field (e.g., Courtney et al., 2022; Hammar et al., 2013) and laboratory flume-study experiments (e.g., Amaral et al., 2015; Berry et al., 2019; Bevelhimer et al., 2019; Castro-Santos & Haro, 2015; Yoshida et al., 2020, 2021). Although valuable, these studies are constrained in their assessment of fish approach due to limitations in their experimental designs such as relying on short time-based trials and sensor capabilities. In the natural environment, Shen *et al.* (2016) found evidence suggesting that a fish's initial opportunity to avoid MRE devices occurs at approximately 140 m during flood tide. In our model, the zone of influence represents this 140 m range in which fish can detect and respond to a turbine and predicts whether a fish's approach will result in a close fish-turbine interaction or avoidance behavior. Recent research also highlights interactions at closer distances, with several studies suggesting that fish exhibit evasive behaviors (e.g., Hammar et al., 2013; Viehman & Zydlewski, 2015). Our model identifies entrainment as the fish-turbine encounter area, which is dependent on turbine size and archetype. Estimates of fish presence within the entrainment component in Admiralty Inlet are lower than those within the zone of influence, indicating fish avoidance as they transition from one area to the other. As an analogy, studies by Bevelhimer *et al.* (2017) and Viehman & Zydlewski (2015) used DIDSON acoustic cameras (Belcher et al., 2002) to capture interactions between fish and turbines. Bevelhimer *et al.* (2017) monitored fish interactions with an axial-flow turbine for over 20 days in East River, NY, finding evidence that 12.5% of fish adjusted their swimming direction and velocity when approaching the operating turbine. Similarly, Viehman & Zydlewski (2015) employed two DIDSON cameras to observe fish behavior around a cross-flow turbine, where 15.5% of fish schools avoided the device by passing above, below, or through the turbine (Viehman & Zydlewski, 2015).

The impact phase of the model includes subevents of collision, blade strike, and collision and blade strike. Probabilities of fish-turbine interaction assuming no avoidance predict higher estimates than scenarios where avoidance is considered. Analogous studies found impact probabilities in models with no avoidance (e.g., Wilson et al., 2006) result in higher values by one to two orders of magnitude compared to our model predictions that include avoidance. In our model, Yoshida *et al.'s* (2021) fish-turbine blade strike probabilities predict lower impact estimates when combined with an avoidance scenario. Yoshida *et al.'s* (2021) lower probability values are attributed to a slower turbine blade rotational speed to fish swimming speed ratio, resulting in greater avoidance and lower blade strike rates. In contrast, our model predicts higher blade strike estimates when coupled with Romero-Gomez & Richmond's (2014) blade strike model that does not include fish avoidance. After review, our range of impact estimates demonstrate that avoidance is an important factor influencing potential interactions, both as a scenario within the model and experimentally with fish and a turbine present.

Admiralty Inlet offers dynamic tidal channels favorable for tidal energy development. While we had some field data from Admiralty Inlet, at the time of data collection there were no hydrokinetic devices deployed in Admiralty Inlet. Fish density data used in probability calculations lack information on fish-turbine interactions, necessitating the use of published avoidance and blade strike values. Use of published literature supports conditional probability values which are calculated using empirical acoustic transect data along sequential steps. The data serve as a series of spatiotemporal snapshots of fish distributions but do not explicitly include individual fish trajectories as they pass through a model domain. Although Admiralty Inlet boasts a diverse species composition, Pacific herring was the primary focus of this study because of their dominant representation within the trawl catch data (Horne et al., 2013). Representing a mixed fish

community by a single species in the conversion of acoustic backscatter measurements to density and abundance estimates is potentially biased, but biases in the data are assumed constant. Pacific herring are used to represent pelagic, schooling fish that are common constituents of any fish community at an MRE site. The model's adaptability allows for examination of culturally significant fish species in the region, acknowledging that other marine species, such as marine mammals, may raise regulatory concerns (Copping & Hemery, 2020). Nevertheless, estimating impact probabilities for Pacific herring in Admiralty Inlet emphasizes utilization of acoustic data and highlights existing data gaps that must be addressed to obtain accurate statistical-based encounter-impact probabilities.

Numerical modeling is a tool used to quantify information gaps and estimate uncertainties to contribute to additional research and monitoring (Buenau et al., 2022). However, models are still affected by lack of information available to accurately validate potential interactions. The construction of the encounter-impact model consists of a combination of empirical data from Admiralty Inlet and literature values. To obtain probability estimates that are validated, ideally, the entire structure of the model should be parameterized with empirical data obtained from the field with a tidal turbine device present. The potential risk of an individual colliding with a stationary component of a device or colliding then being struck by a turbine blade has not been studied in field or laboratory-based research. This area of direct, potential impacts should be prioritized when developing future fish-turbine monitoring studies as it can be labeled a likely interaction for larger MRE structures. The current model also lacks additional possibilities of impact that should be considered, such as hydraulic shear stress (Cada et al., 2007) and barotrauma (Brown et al., 2012). Flume studies are one opportunity to examine hydraulic conditions when fish are entrained with the turbine, yet it can be difficult to monitor whether fish would have an

immediate effect from the turbine itself or flume hydraulics (Castro-Santos & Haro, 2015). Our model does not consider the possibility of what might happen to a fish after it has interacted with a turbine in the form of a collision and/or blade strike. Effects from impact might include fish injury, mortality, or population displacement (Copping et al., 2021, 2023). Fish mortality and population displacement can be labeled as delayed impacts, where long-term effects of fish-turbine interactions are not observed immediately. Broadening knowledge of these direct and delayed impacts is a crucial first step in environmental assessment, especially when estimating interactions between individual species with a single device (Copping et al., 2023).

Moving forward with data collection, model adaptation, application, and validation to estimate potential impacts, we must consider factors that can contribute to high-risk estimates. Probabilities of encounter and impact are highest at night (e.g., Viehman & Zydlewski, 2015; Williamson et al., 2019). Turbine design is another factor that contributes to higher probability estimates of impact. A turbine with greater dimensions, like the approximate 30 m by 10 m TidGen cross-flow turbine (Shen et al., 2016), has a greater chance for fish to interact with the device. Compared to the dimensions of the Verdant Power KHPS axial-flow turbine (Bevelhimer et al., 2017) used in this study, a cross-flow turbine is six times larger than an axial-flow turbine. The empirical data estimates show higher probabilities of entrainment and collision for the cross-flow turbine, most likely due to the amount of space the device is taking in the water column. Ultimately, when collecting empirical data on animal-turbine interactions, results of this study support monitoring potential impacts for day and night continuously, as well as the two different types of turbine structure. By considering these different factors, data collection will entail a more inclusive outlook of empirically-based encounters and impacts.

Chapter 3. Using an agent-based model to examine the effects of avoidance and aggregation behavior on fish-turbine interactions

3.1 Introduction

Marine Renewable Energy (MRE) has the potential to produce low-carbon energy from the movement of ocean currents or waves, and to contribute to sustainable economic development (Cavagnaro et al., 2020). However, there are concerns about environmental impacts such as disruption to marine ecosystems from tidal energy devices that affect marine life (Hemery et al., 2021). The most effective way to understand full potential of tidal energy generation and its impact on marine ecosystems is by studying operational large-scale commercial arrays (Hasselman et al., 2023). In North America, the lack of commercial-scale tidal arrays is primarily due to government regulations, which hinder investment and development. These regulatory challenges have slowed development of tidal energy sites, with only a few commercial scale arrays occurring internationally, primarily in Europe and parts of Asia (Copping et al., 2020a).

Due to the limited number of operational tidal turbine sites, current efforts employing physical, statistical, and simulation models to quantify risks that tidal turbines pose to ecosystems are limited. Of those that investigate effects on fish, most studies often ignore fish behavior in changing environmental conditions (Gill, 2005). Experimental flume studies (e.g., Amaral et al., 2015; Berry et al., 2019; Castro-Santos & Haro, 2015) simulate water flows around tidal devices, allowing researchers to observe and measure potential detrimental effects on individual fish as they encounter and interact turbine prototypes. However, they lack real-world applicability, as these controlled conditions cannot fully replicate tidal site water flow dynamics. Statistical models use empirical data to observe characteristics of animal spatial distributions around MRE devices without making assumptions about their positions or behaviors. These models are used to estimate

potential animal-turbine encounter and interactions, but often cannot be applied to other MRE sites due to location, time, and condition specificity of empirical data. Statistical models, such as the Collision Risk Model (CRM) (Band, 2012; Band et al., 2016) and Encounter Rate Model (Wilson et al., 2006), typically include a subset of factors affecting encounter and interaction estimates. These models have also been formulated for sites with axial-flow turbines and do not include behavioral responses relevant to MRE encounters (e.g., device avoidance and animal aggregation). Simulation models provide an efficient approach to predicting potential animal-turbine interactions without incurring financial, ethical, or ecological costs. Specifically, agent-based models (ABMs), can be used to simulate scenarios by modifying tidal flows, animal swimming, and animal behavior (e.g., Grippo et al., 2020; Rossington & Benson, 2020). However, simulation models are simplified representations of reality, that are constrained by the number and complexity of variables they incorporate.

Simulation tools also serve as an alternative to data-limited statistical approaches by generating predictions that complement or extend empirical datasets (An et al., 2021). ABMs are flexible tools that can simulate actions of individuals or agents within a population that follow a set of behavioral rules. These models can be parameterized using data from field observations, existing datasets, or published values (Murphy et al., 2020), where each agent is parameterized with a set of traits that influence their interactions with other agents and the environment (DeAngelis & Mooij, 2005). The model framework allows agents to perceive and respond to their environment, other agents, and obstacles (McLane et al., 2011; Rose et al., 1999). ABMs can incorporate and evaluate factors that cannot be explicitly examined in statistical models, as ABMs parameterized with sufficient empirical data can capture the combined effects of all conditions.

We developed a four-dimensional (i.e., three spatial dimensions over time) ABM that includes all components from the encounter-impact model (c.f. Figure 1, Chapter 2) and integrates site, physical, and biological factors to analyze approach and potential interaction between fish and tidal turbines. The structure of the model includes MRE site characteristics, a large spatial domain, fluctuating tidal speeds, and animal-device interactions. This study aims to build an agent-based simulation model to estimate encounter and impact probabilities for individual and aggregations of fish, conduct a sensitivity analysis of fixed parameter values, and to compare magnitudes of agent-based probabilities to statistical probabilities.

3.2 Methods

3.2.1 *Spatial environment*

The encounter-impact, agent-based simulation computes probabilities of fish approaching and potentially interacting with model spatial components and two different tidal turbine types in a three-dimensional environment over time (Figure 1; Figure 2A, B). Within the model domain, the dimension parallel to tidal flow (*x*-axis) is 400 meters (m) (i.e., approximately double the length of model components and turbine), the horizontal dimension orthogonal to the tidal flow (*y*-axis) is set at 100 m, and water depth (*z*-axis) is set at 55 m (which is analgous to the tidal turbine site at Admiralty Inlet, WA, USA; Horne et al., 2013) (Figure 3). Other than the turbine, model spatial volumes have no influence on fish trajectories and are only used in tabulating fish presence for probability calculations (c.f. Chapter 2.2.1). Periodic boundary conditions define a cyclic state of flow across boundary surfaces and are applied along the *y*-axis where fish can enter at one end of the *y*-axis and exit at the other end. Periodic boundary conditions are not applied to the *x*- or *z*-axes. The *x*-axis allows fish to exit either end of the domain without re-entering the environment. The *z*-axis (i.e., the top and bottom boundaries of the domain) uses reflective boundary conditions

to prevent fish from exiting the environment. Fish that encounter these boundaries are reflected back into the domain at the same incident angle resulting in retention within the simulated volume.

The model includes unidirectional tidal flow in the positive *x*-direction, where velocities range from 0 to 3.0 ms^{-1} (as observed at Admiralty Inlet, WA, USA; Horne et al., 2013) (Figure 3). Tidal velocities from 0 to 0.25 ms^{-1} do not restrict fish active locomotion, which allow fish to swim in all directions with little influence from tidal flow. Tidal velocities exceeding 0.25 ms^{-1} represent passive locomotion, or drifting, where current flow exceeds maximum fish swimming speed. A tidal flow of 0 ms^{-1} enables fish to move independently of the water. The model characterizes a full tidal cycle, but probability calculations exclude negative tidal velocities (i.e., where flow direction moves right to left) since a negative flow exceeding 0.25 ms^{-1} prevents fish from encountering the turbine. Within the model, results from the second half of a tidal cycle (i.e., negative tidal velocities with fish swimming right to left) will parallel those in the positive direction.

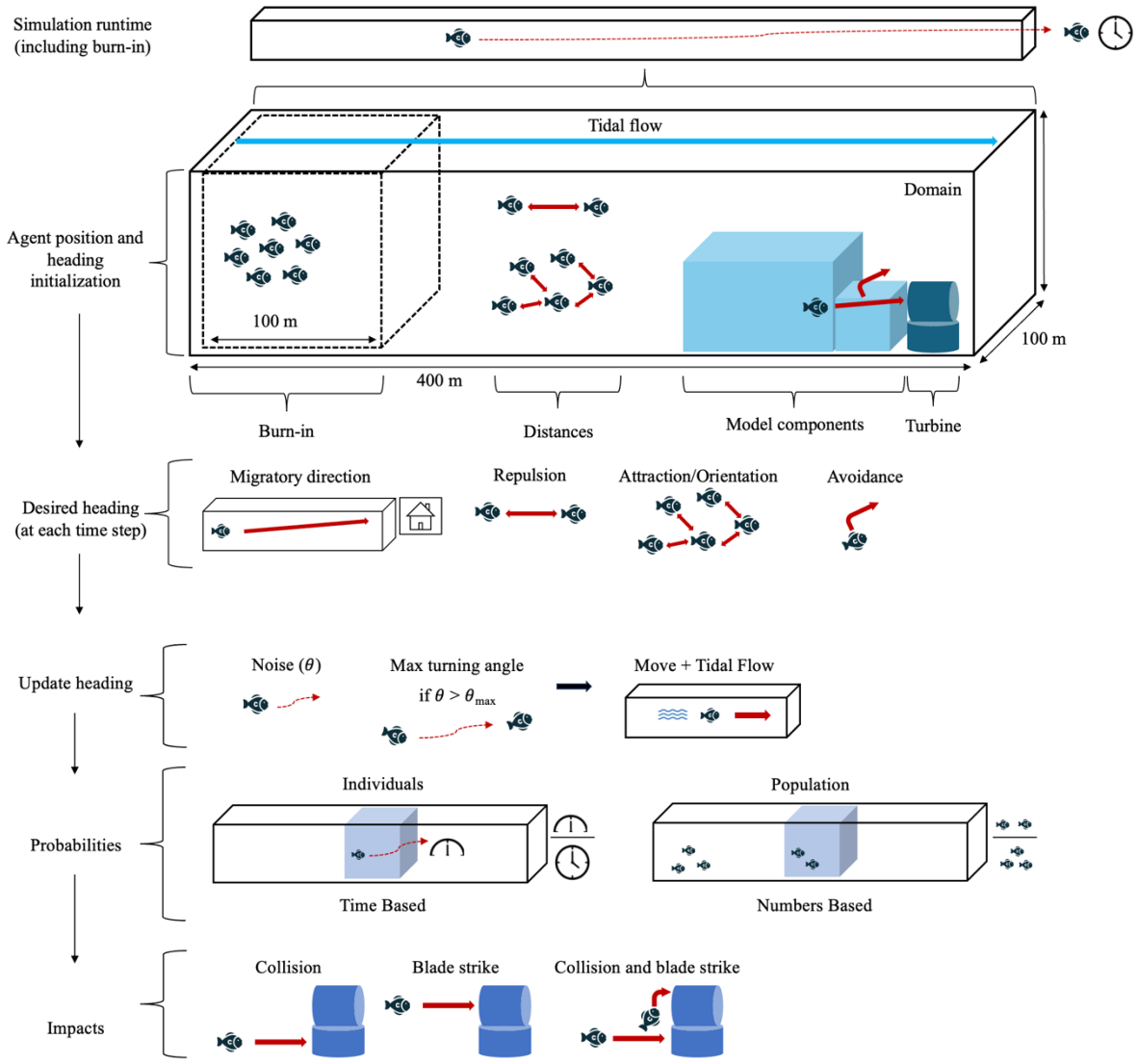

Figure 3. A schematic of the overall agent-based model structure including domain size, agent initialization, agent behavior, computation of probability estimates, and types of potential impacts.

3.2.2 *Tidal turbines within the spatial environment*

Three-dimensional footprints of representative axial and cross-flow tidal turbines are modeled in this study. Axial-flow turbine dimensions are based on the Verdant Power Kinetic Hydropower System (Bevelhimer et al., 2017), while cross-flow turbine dimensions are based on

the Ocean Renewable Power Company TidGen Power System (Shen et al., 2016). For the axial-flow turbine, the turbine base is modeled as a cylinder with a height and a radius of 5 m. The upper portion is also cylindrical, with the same 5 m height and radius to match the turbine base but oriented horizontally (*y*-axis) with the circular ends pointing to the left and right (see example in Figure 3). The cross-flow turbine is also modeled with both the base and the upper portion as cylinders. The base has a height of 15 m and a radius of 10 m, while the blade radius height is 10 m to match the turbine base. Turbine placement in the model is adjacent to the entrainment model component volume at approximately (*x*-375, *y*-50, *z*-0) on the right side of the environment.

3.2.3 *Fish and Migration*

Pacific herring (*Clupea pallasii*, hereafter herring) undergo annual feeding and spawning migrations and form aggregations through their annual movement cycle (Huse et al., 2002). Misund (1993) collected data from a multi-beam acoustic sonar and found that herring tend to swim alongside others of similar body lengths and in shallow waters up to 60 m deep. Agents (i.e., individual fish) within the simulation are modeled to reflect herring behavior and physiology. Assigned traits and rule-based behaviors govern agent interactions with their neighbors and the environment. Consequently, fixed parameters chosen in Table 4 reflect herring behavior and school size.

Table 4. Fixed parameter values and experimental factors for the agent-based, encounter-impact model.

Parameter	Value
Migratory direction weight	0.2 ± 0.04
Repulsion distance (m)	2 ± 0.4
Attraction distance (m)	15 ± 3
Alignment distance (m)	10 ± 2
Attraction and alignment weight	0.2 ± 0.04
Avoidance strength, *k*	-0.1 ± 0.02
Maximum turn angle (radians)	0.8 ± 0.16
Turn noise scale (radians)	0.01 ± 0.002
Swimming speed (bls^{-1})	1

Within the model domain, herring swimming direction is influenced by a migratory direction, with a preferred bearing (Bernardi & Scianna, 2020) in the positive *x*-direction. Migratory direction is the highest behavioral priority among all behavioral components in the model (Figure 3), influencing the net direction of individual fish. Equation (3.1) defines the migratory direction of an individual fish, indexed by *i,* at each time step $t + 1$:

$$\text{Direction}_{\text{migratory}_i}(t + 1) = \text{Direction}_{\text{migratory}_i}(t) + \alpha \cdot (1, 0, 0) \quad (3.1)$$

where migratory direction is based on the fish's current direction at its current time step *t*, modified by a weight parameter, $\alpha = 0.2$ (Table 4), that determines the change in direction in the positive *x*-direction (Couzin et al., 2005). The weight parameter, α, is multiplied by (1, 0, 0), which is a unit

vector in three-dimensional space where 1 indicates its magnitude in the *x*-direction and 0 indicates no magnitude in the *y*- and *z*-directions.

3.2.4 *Fish social interactions*

Herring movement is based on the zonal schooling model described in Couzin *et al.* (2002, 2005). Aggregation behavior incorporates repulsion, attraction, and alignment forces within specified radii of each fish (Reynolds, 1987). Among these three forces fish to fish repulsion is prioritized, where each individual fish, with the position of each fish indexed by *i*, maintains a separation from their neighbors, whose positions are indexed by *j*, within a zone of repulsion. The repulsion force minimizes collisions among individuals (Figure 4). Equation (3.2) defines a normalized repulsion vector for each fish based on surrounding neighbor within the repulsion zone at each time step *t*:

$$\text{Repulsion}_i\,(t+1) = \sum_{j \neq i} \frac{-\left(\text{position}_i - \text{position}_j\right)}{\| \text{position}_i - \text{position}_j \|} \tag{3.2}$$

where the total repulsion force for each fish is the sum of individual repulsion forces from each neighbor within the repulsion zone. Attraction and alignment forces govern how fish move as a cohesive group (Aoki, 1982). The attraction force is the inclination of fish to move towards each other, and the alignment force orients their direction of movement with nearby neighbors (Figure 4). To determine the strength of attraction and alignment forces, a weighted attraction and alignment term, ω, is used to balance the two forces, where a value of 1 equals maximum attraction and a value of 0 denotes maximum alignment (Couzin et al., 2005). Equation (3.3) summarizes the combined influence of attraction and alignment forces:

$$\text{Attraction \& Alignment}_i\,(t+1) = \sum_{j \neq i} \omega \cdot \frac{\left(\text{position}_i - \text{position}_j\right)}{\| \text{position}_i - \text{position}_j \|} + (1 - \omega) \cdot \frac{\left(\text{heading}_j\right)}{\| \text{heading}_j \|} \tag{3.3}$$

where a normalized attraction vector and normalized alignment vector (i.e., heading direction) is calculated for each neighbor. The total force on each fish i at each time step t is the sum of individual attraction and alignment vectors from each neighbor within the zone of attraction and zone of alignment, with a weighted term, $\omega = 0.2$ (Table 4), set to match tight herring schooling formations that are often disc-shaped and spherical (Misund, 1993). The resultant schooling force governing the direction of fish at time $t + 1$ is the total of all forces at the current time step t:

$$\text{Schooling}_i\,(t+1) = [\beta \cdot \text{Attraction \& Alignment}_i\,(t)] + \text{Repulsion}_i\,(t) \tag{3.4}$$

where equation (3.4) includes a schooling parameter, β, ranging from 0 to 1, which influences the degree of schooling behavior. A value of 0 signifies asocial behavior (individuals act independently) and a value of 1 denotes a stronger tendency towards attraction and alignment forces.

$$\text{Repulsion}_i\,(t+1) = \sum_{j \neq i} \frac{-(\text{position}_i - \text{position}_j)}{\| \text{position}_i - \text{position}_j \|}$$

$$\text{Attraction \& Alignment}_i\,(t+1) = \sum_{j \neq i} \omega \cdot \frac{(\text{position}_i - \text{position}_j)}{\| \text{position}_i - \text{position}_j \|} + (1-\omega) \cdot \frac{(\text{heading}_j)}{\| \text{heading}_j \|}$$

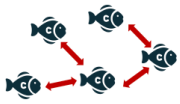

$$\text{Avoidance}_{i,\,\text{turbine}}\,(t+1) = \begin{cases} 0 & \text{if distance} > 140 \\ e^{\frac{-\,\text{distance}}{k}} & \text{if distance} \leq 140 \end{cases}$$

Figure 4. Schooling behavior including a migratory direction, noise and maximum turning angle equations, and turbine avoidance equations.

3.2.5 *Fish avoidance behavior*

Turbine avoidance by fish is defined as a change in a fish's trajectory in response to tidal devices (Bender et al., 2023; Berry et al., 2019; Hammar et al., 2013). Active avoidance involves fish swimming to evade model components or the turbine. Passive avoidance occurs as fish drift through model components or the turbine, where trajectories are influenced by tidal speed. Initiation of fish-turbine active avoidance at each time step t occurs at distances less than 140 m (c.f., Shen et al. 2016), with an amplitude inversely proportional to the distance between a fish, indexed by i, and the turbine's base or blade (Figure 4). Equation (3.5) models fish avoidance behavior as an exponential decay function relative to the distance from a turbine:

$$\text{Avoidance}_{i,\,\text{turbine}}\,(t+1) = \begin{cases} 0 & \text{if distance} > 140 \\ e^{\frac{-\,\text{distance}}{k}} & \text{if distance} \leq 140 \end{cases} \tag{3.5}$$

where k is the amplitude of avoidance strength and *distance* is the distance between a fish and the turbine. If the distance between a fish and a turbine exceeds 140 m, then no avoidance behavior occurs.

3.2.6 *Combining all behavioral forces*

Updated positions and headings of each fish at time step $t + 1$ are determined by combining migratory direction (Eq. 3.1), aggregation (Eq. 3.2-3.3), and avoidance behavior (Eq. 3.5) into a single equation:

$$(\text{Position} + \text{Heading})_i\,(t+1) = \text{Position}_i\,(t) + \alpha \cdot (1, 0, 0) +$$

$$\sum_{j \neq i} \frac{-(\text{position}_i - \text{position}_j)}{||\,\text{position}_i - \text{position}_j\,||} + \left[\beta \cdot \left[\sum_{j \neq i} \omega \cdot \frac{(\text{position}_i - \text{position}_j)}{||\,\text{position}_i - \text{position}_j\,||} + (1 - \omega) \cdot \frac{(\text{heading}_j)}{||\,\text{heading}_j\,||}\right]\right]$$

$$+ \begin{cases} 0 & \text{if distance} > 140 \\ e^{\frac{-\,\text{distance}}{k}} & \text{if distance} \leq 140 \end{cases} \qquad (3.6)$$

Random noise in positions and headings is introduced at each time step to add variability in individual fish trajectories (Codling et al., 2008; Li et al., 2009) (Figure 3). In equation (3.7), the dot product is used to calculate the angle difference, $\theta_{\Delta\,\text{heading}_i}$, between the fish's current heading at time t and its updated heading at $t + 1$ after incorporating random noise (0.01 radians, Table 4).

$$\theta_{\Delta\,\text{heading}_i} = \cos^{-1}\left(\frac{(\text{Heading}_i(t) \cdot (\text{Heading} + \text{Noise})_i(t+1))}{(||\text{Heading}_i(t)|| \cdot ||(\text{Heading} + \text{Noise})_i(t+1)||)}\right) \qquad (3.7)$$

To prevent fish from making excessive directional changes at each time step $t + 1$, the maximum turning angle is restricted to 0.8 radians (approximately 45 degrees) (Table 4) (Figure 3). The choice of 0.8 radians is supported by the experimental studies of Domenici & Blake (1997) who

found maximum turning angles for pelagic fish ranged between 45 to 50 degrees. Each fish's heading is calculated by comparing the angle between the current and updated headings:

$$\text{Heading}_i\,(t+1)=$$

$$\begin{cases} \mathrm{v}(t)\cdot\cos(\theta_{\max})+\left(\dfrac{\mathrm{v}(t)-(\mathrm{v}(t+1)\cdot\mathrm{v}(t))\cdot\mathrm{v}(t)}{\|\mathrm{v}(t+1)-(\mathrm{v}(t+1)\cdot\mathrm{v}(t))\cdot\mathrm{v}(t)\|}\right)\cdot\sin(\theta_{\max}) & \text{if } \theta_{\Delta\,\text{heading}_i} > \theta_{\max} \\ (\text{Heading}+\text{Noise})_i & \text{else} \end{cases} \tag{3.8}$$

If the desired turning angle exceeds the maximum turn angle, then the fish's heading is adjusted by rotating the initial heading vector, v(t), towards the desired heading vector, v(t + 1) by the maximum allowable angle. If the desired heading is within the allowable range ($\theta \leq \theta_{max}$), then the desired heading is updated with a degree of randomness, represented by $(\text{Heading} + \text{Noise})_i$ (Eq. 3.8) (Figure 4).

3.2.7 *Distances between neighboring fish and the tidal turbine*

To determine whether individual fish are interacting with their neighbors and/or a tidal turbine from their current position, we calculate distances between them to find whether we apply behavior forces described in 3.2.4 or turbine avoidance described in 3.2.5. Fish to neighboring fish distances are computed using the Euclidean distance formula in a three-dimensional space:

$$D_{i,j} = \sqrt{(x_i - x_j)^2 + (y_i - x_j)^2 + (z_i - x_j)^2} \tag{3.9}$$

where $D_{i,j}$ is the calculated distance between an individual fish, i, and a neighboring fish, j (Figure 5). The distance between a fish and the turbine base is calculated using the Euclidean distance formula (Equation 3.9), with $D_{i,turbine}$ being the distance between fish and the turbine base, representing individual fish coordinates at their current position (x_i, y_i, z_i), and the turbine base at fixed coordinates (375, 50, 5) for an axial-flow turbine and (375, 50, 15) for a cross-flow turbine.

To calculate the distance between a fish and the turbine rotor, we use the center of the turbine's cylindrical face represented by the coordinates ($x_{turbine}$, $y_{turbine}$, $z_{turbine}$) (see example of turbine face in Figure 5). This calculation involves two main components: the turbine face distance in the *x*-direction (Eq. 3.10) and the radial distance in the *y*-*z* plane (Eq. 3.11).

$$\text{Turbine face distance} = || x_i - x_{turbine} || - \frac{\text{turbine height}}{2} \tag{3.10}$$

$$\text{Radial distance} = (y_i - y_{turbine})^2 + (z_i - z_{turbine})^2 \tag{3.11}$$

$$D_{i,\text{turbine}} = \begin{cases} \text{Turbine face distance}, & \text{if radial distance} \leq r \\ \sqrt{(\text{Turbine face distance})^2 + (\text{Radial distance})^2}, & \text{if radial distance} > r \end{cases} \tag{3.12}$$

where *r* is 5 m for the radius of the axial turbine and 10 m is the radius of the cross-flow turbine. The turbine face distance (Eq. 3.10) is the absolute difference between the fish's and turbine's *x*-coordinates, adjusted by half the turbine's height. The radial distance (Eq. 3.11) is the squared difference between the fish's and turbine's *y*- and *z*-coordinates. The final distance, $D_{i,turbine}$, is a piecewise function (Eq. 3.12). If the radial distance is less than or equal to the turbine's radius *r*, the final distance is the turbine face (Eq. 3.10). If the radial distance exceeds *r*, the final distance is the Euclidean distance combining the turbine face (Eq. 3.10) and radial distances (Eq. 3.11) (Figure 5).

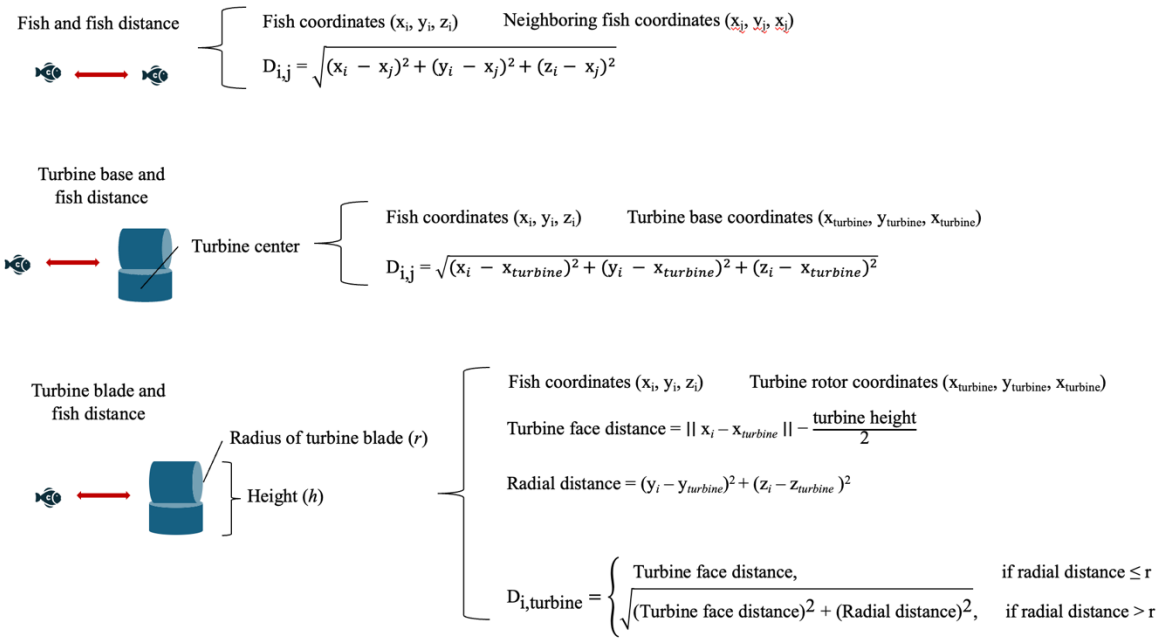

Figure 5. Distance equations between fish and neighboring fish and between fish and turbine structures.

3.2.8 *Fish movement*

Fish movement is characterized by a constant swimming speed of 1 body length per second (He, 1993) (Table 4), which is within the range of fish aerobic swimming. In equation (3.13), fish position and bearing at the next time step, $t + 1$, is based on current position at time t, swimming speed and updated heading at time t, and tidal influence including speed and direction:

$$(\text{Position} + \text{Heading}_i)(t+1) = \text{Position}_i(t) + \left[\text{Speed}_i \cdot \text{Heading}_i(t)\right] + [\text{Tidal speed} \cdot (1,0,0)] \quad (3.13)$$

3.2.9 *Fish initialization within the domain*

Fish are initialized in the domain with random starting positions (x_i, y_i, z_i) and orientations $\left(\theta_{\text{heading}_i}\right)$. The initial numbers of fish aggregations are randomly allocated using a constant density, ρ, and a dimensionless scaling factor, *F* that determines the number of aggregations:

$$\text{Number of aggregations} = F \cdot \sqrt[3]{\rho} \tag{3.14}$$

At a constant density ρ, a larger *F* value (e.g., 5) results in more numerous but smaller fish aggregations. Conversely, decreasing the *F* value (e.g., 2) leads to fewer, yet larger fish aggregations. Fish are initialized in a 55 by 100 by 55 m burn-in volume at the left end of the model domain (Couzin et al., 2005), where fish spend approximately 5% of the total simulation runtime in this volume to swim and form initial schools.

3.2.10 *End conditions of simulation run*

Each simulation is considered an individual run, beginning when fish are initialized within the burn-in volume and ending when all fish in the domain exit the environment from either the right or left side (*x*-axis). After the final fish exits the model domain, the total number of time steps is tabulated, and the simulation is restarted for the next run (Figure 3).

3.2.11 *Data acquisition from simulation runs*

Interactions between fish and tidal turbines can include collisions and/or blade strikes (c.f. Chapter 2, Peraza & Horne, 2023) (Figure 3). Within the model, a fish will react to the turbine based on their distance to the device and fish-turbine avoidance (Equation 3.5). If a fish does not evade a device, then a fish can collide with a stationary component of the turbine. Once a collision

has occurred, the fish's bearing in the next time step is determined by the vector originating from its current position extending towards the turbine's location, which is used to determine the direction and strength of a rebound at a mirrored incident angle. Blade strikes occur when a fish enters the upper half of the turbine structure, where fish are randomly assigned a probability of being struck or passing through turbine blades. Probabilities of blade strike range from 0.02 (Yoshida et al., 2020, 2021) to 0.13 (Courtney et al., 2022). When a fish enters the turbine rotor-swept area, the number of time steps spent inside this area is tabulated, and individuals are assigned a random probability of escapement. If this probability is less than or equal to 0.11, a blade strike occurs, and then the fish continues their current trajectory. If the probability of escapement is greater than 0.11, then the fish avoids interacting with the turbine blades and passes through.

Probabilities of encounter and impact are computed for individuals within a population, and for all fish in the simulation as a population (Figure 3). Individual probability values are calculated using the time each fish spends in each model component volume and the turbine. Probabilities are determined by counting fish duration (i.e., number of time steps) in each volume component, divided by the duration of the simulation. The total number of time steps varies in each simulation run, as the model runs until the last fish is no longer in the model domain. Fish population probabilities are based on the number of fish that end up in each volume component. These population probability estimates are based on the summation of fish counts in each volume component, divided by the total number of fish in the simulation. Fish-turbine impacts are calculated for the population by dividing fish count occurrences by total fish abundance, where the turbine upper section is the turbine rotor-swept area that results in a blade strike or pass through, and the lower portion of the turbine as a stationary base. In addition to calculating fish presence probabilities for each model component and the turbine (Figure 1), the time individual fish spend

within the rotor-swept area and the number of fish entering this area is recorded to assess how quickly fish escape once inside the rotor area. The average amount of time an individual fish spends within each model component and the average proportion of fish in the population who encounter model components is also calculated.

3.2.12 *Experimental structure*

The simulation can be used to examine the relative importance of different factors influencing animal-turbine interactions (Figure 3). Three experimental factors are analyzed: 1) fish abundance, 2) fish aggregation behavior, and 3) tidal flow speed (Figure 6). To explore how the density of individuals in the model domain influences aggregation and turbine avoidance, a baseline number is set to 328 fish. This number is based on the catch of Pacific herring from 36 mid-water trawls conducted in Admiralty Inlet (Horne et al., 2013). The effect of density change is examined by doubling the value to 656 fish in one set of simulations and halving the value to 164 fish in a second set of simulation runs (Table 4; Figure 3).

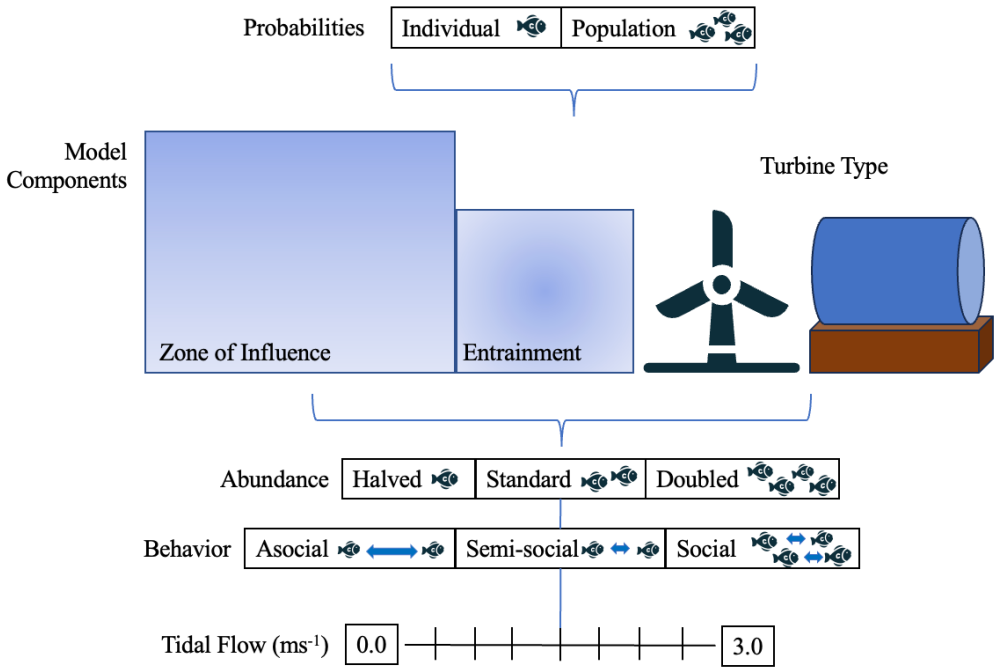

Figure 6. A schematic of the experimental design for simulation runs. Probabilities are computed for individual fish and populations. Probabilities are computed for each model component and turbine design, where the simulation's structure is shaped by component and turbine characteristics. Experimental factors investigated in simulation runs include fish abundance (categorical), aggregation behavior (categorical), and tidal flow (continuous).

Levels of fish social interaction that potentially impact dynamics of fish aggregation and their encounters with the turbine are also examined. The aggregation weight parameter is varied across three levels (0, 0.5, 1) to represent asocial, semi-social, and social fish aggregation behaviors (Table 4, Figure 3). Asocial behavior does not include an attractive force among fish, resulting in independent fish trajectories. The semi-social scenario results in the formation of multiple, small aggregations of fish. The highest level of social behavior includes a rapid formation of a cohesive single aggregation.

The final experimental factor investigated is tidal flow, a factor that determines a fish's ability to swim independent of water motion in a dynamic environment. Tidal speeds are increased

by 0.25 ms^{-1} increments from 0 to 1 ms^{-1} to examine fish behavior at slower tidal speeds. Tidal speeds beyond 1 ms^{-1} are increased by 0.5 ms^{-1} to examine fish behavior at higher speeds. This tidal range enables a detailed examination of how incremental increases in flow influences encounter-impact probabilities (see Table 4, Figure 3). Model parameters listed in Table 4 are held constant at their base values, while remaining experimental factors (i.e., abundance, aggregation behavior, flow speed) are systematically varied through each factor level in sets of 1000 simulations.

3.2.13 *Sensitivity analysis*

The choice of factors and parameter values within an agent-based model can potentially influence the outcome of each simulation run and corresponding metrics derived from simulations. Parameter values that influence fish behavior in the simulation are based on empirical data, literature values, or biological reasoning (e.g. physiological limits) but ultimately are assigned arbitrarily (Table 4). A sensitivity analysis is used to quantify the impact of parameter value choices and the relative magnitude of parameter effects. Results from a sensitivity analysis can also be used to identify important empirical data streams that are needed to evaluate and validate parameter value choices in simulation models (Frey & Patil, 2002). A local sensitivity analysis (Saltelli, 2004) examines model sensitivity around a set of parameter values, with a ± 20% change from an initial value. One parameter is adjusted based on the ± 20% change while remaining parameters are set to baseline values (Table 4). Sensitivity analyses simulations are run 1000 times for each ± 20% parameter change. Probabilities for each parameter change are expressed as a 95% confidence interval, where results are presented as the percent change deviation from the lower and upper confidence bounds (Saltelli, 2008).

3.2.14 *Analysis between statistical and simulation model*

A comparison of results between the statistical (c.f. Chapter 2.3) and agent-based (c.f. Chapter 3.3) modeling approaches enables an examination of the structure of the encounter-impact model (Figure 1). The statistical model uses animal density and distribution data along with published blade strike values but does not incorporate population fish-turbine interactions or avoidance. To compare probability estimates, average probabilities, based on their respective sample sizes, are tabulated by model type (i.e., statistical or simulation), model component (e.g., zone of influence, entrainment), and turbine type (i.e., axial-flow, cross-flow).

Following the calculation of average encounter-impact probabilities from the simulation model, a non-parametric Wilcox T-test (Wilcoxon, 1945) is used to compare the means of paired groups. In this case, the mean probabilities are compared for each model component and each model type.

3.3 Results

Probability of occurrences are obtained for individuals and populations of fish organized by model component, turbine design, fish abundance, aggregation behavior, and tidal flow (Figure 6). As expected, based on the dimensions of model components (Figure 1), more fish enter the zone of influence than any other model component, with up to 40% of fish entering this zone. A much smaller proportion of fish physically contact the turbine, with collision and blade strike probabilities never surpassing 0.0025 across all model configurations.

3.3.1 *Effects of fish abundance*

Varying fish density over a factor of four has no effect on the amount of time individual fish spend within the zone of influence, entrainment, and turbine rotor-swept area model

components (Appendix A3.1, A3.3, A3.5). Overall, individual fish spend up to 50% of their time within the zone of influence, up to 25% of their time within the entrainment component, and up to 3% of their time within the turbine rotor-swept area (Appendix A3.1, A3.3, A3.5).

Similarly, there is no difference in the proportion of the fish population, that interacts with model components across densities. Instead, across all fish abundances, as fish approach each model component their risk of interacting with components or the turbine decreases. Based on the average probabilities in Table 5 and Appendix A3.7 and A3.8, fish are more likely to collide with the turbine than be struck by a turbine's blade. Fish populations are also less likely to interact with an axial-flow turbine than a cross-flow turbine among the three fish abundances (Table 5).

Table 5. Summary table of average agent-based, encounter-impact population probability estimates comparing fish abundance.

Fish Population Probabilities			
Fish abundance (number of individuals)	Model Components	Axial-Flow	Cross-Flow
164 fish	Zone of Influence	0.1212	0.3247
	Entrainment	0.07531	0.2382
	Collision	0.0004778	0.01468
	Turbine Rotor Entry	0.0001323	0.02075
	Blade strike	0.00001377	0.002392
	Collision and blade strike	0.000001806	0.0001741
328 fish	Zone of Influence	0.1190	0.3663
	Entrainment	0.07475	0.2588
	Collision	0.0003404	0.01484
	Turbine Rotor Entry	0.0001148	0.03077
	Blade strike	0.00001422	0.003779
	Collision and blade strike	0.000001242	0.0003562
656 fish	Zone of Influence	0.1258	0.3803
	Entrainment	0.08190	0.2700
	Collision	0.0008459	0.009181
	Turbine Rotor Entry	0.0001696	0.03419
	Blade strike	0.00005043	0.004290
	Collision and blade strike	0.000003240	0.0001959

3.3.2 *Effects of aggregation behavior*

When comparing effects of aggregation behavior on the amount of time individual fish spend within the zone of influence and the turbine rotor-swept area, asocial fish spend less time (i.e., where individual fish trajectory probabilities are lower) in these areas compared to semi-social and social fish (Appendix A3.1, A3.5). However, fish spend the same amount of time within the entrainment model component among the three aggregation behaviors (Appendix A3.3).

In cases where fish exhibit social behaviors, a higher proportion of the fish population are more likely to encounter model components or interact with the tidal turbine compared to asocial

fish. Under asocial conditions, fish are, on average, 0.045% more likely to collide with an axial-turbine compared to semi-social and social fish. Additionally, asocial fish are 0.3% more likely to collide with a cross-flow turbine than their semi-social and social counterparts (Table 6). Like the comparison of fish densities, asocial and aggregating fish are more likely to interact with a cross-flow turbine than an axial-flow turbine (Table 6).

Table 6. Summary table of average agent-based, encounter-impact population probability estimates comparing fish aggregation behavior.

Fish Population Probabilities			
Aggregation behavior	Model Components	Axial-Flow	Cross-Flow
Asocial behavior	Zone of Influence	0.09312	0.3091
	Entrainment	0.06305	0.2391
	Collision	0.0006238	0.01338
	Turbine Rotor Entry	0.00006063	0.006663
	Blade strike	0.000007452	0.0007498
	Collision and blade strike	0.000001242	0.00005623
Semi-social behavior	Zone of Influence	0.1354	0.3899
	Entrainment	0.08880	0.2551
	Collision	0.00006775	0.009683
	Turbine Rotor Entry	0.0001011	0.03862
	Blade strike	0.00001025	0.004645
	Collision and blade strike	0.0000003871	0.0002873
Social behavior	Zone of Influence	0.1344	0.4060
	Entrainment	0.08221	0.2925
	Collision	0.0003400	0.01169
	Turbine Rotor Entry	0.0002686	0.04860
	Blade strike	0.00002893	0.006225
	Collision and blade strike	0.000002419	0.0003723

3.3.3 *Effects of tidal speed variation*

The amount of time fish spend within model components varies proportionally with tidal speed. Periodic tidal conditions significantly influence this interaction, potentially affecting fish

exposure to tidal turbines. As tidal speed increases, fish spend less time in the zone of influence and entrainment model components compared to slower tidal speeds (Appendix A3.1, A3.3). In contrast, the amount of time fish spend within the turbine rotor-swept area increases as fish transition from active to passive locomotion (Appendix A3.5).

As tidal speed increases, the proportion of fish encountering the zone of influence decreases. However, the opposite is true for the entrainment model volume, where the proportion of fish entrained with the turbine increases as tidal speeds increases. The proportion of fish entering the rotor-swept area and/or being impacted by the turbine through collision and/or blade strikes also increases as tidal speed increases. For an axial-flow turbine, impacts of collision, blade strike, and sequential collision and blade strike occur when tidal speeds exceed 0.25, 1, and 1.5 ms^{-1} respectively. For a cross-flow turbine, impacts of collision, blade strike and sequential collision and blade strike occur when tidal speeds exceed 0, 0.25, and 0.5 ms^{-1} respectively.

Table 7. Summary table of average agent-based, encounter-impact population probability estimates comparing tidal speeds.

Fish Population Probabilities			
Tidal speed	Model Components	Axial-Flow	Cross-Flow
0 ms^{-1}	Zone of Influence	0.1272	0.3883
	Entrainment	0.06221	0.1779
	Collision	0.0000003048	0.0008876
	Turbine Rotor Entry	0	0.000001161
	Blade strike	0	0
	Collision and blade strike	0	0
0.25 ms^{-1}	Zone of Influence	0.1236	0.3767
	Entrainment	0.06896	0.2254
	Collision	0.00002957	0.002252
	Turbine Rotor Entry	0	0.0005078
	Blade strike	0	0.00009581
	Collision and blade strike	0	0.000003484
0.5 ms^{-1}	Zone of Influence	0.1228	0.3718
	Entrainment	0.07116	0.2463
	Collision	0.00003719	0.004099
	Turbine Rotor Entry	0.0000003048	0.002248
	Blade strike	0	0.0004547
	Collision and blade strike	0	0.00002322
0.75 ms^{-1}	Zone of Influence	0.1240	0.3701
	Entrainment	0.07789	0.2624
	Collision	0.00005365	0.006835
	Turbine Rotor Entry	0.0000006097	0.01071
	Blade strike	0.0000003048	0.002043
	Collision and blade strike	0	0.0001004
1.0 ms^{-1}	Zone of Influence	0.1233	0.3676
	Entrainment	0.07946	0.2716
	Collision	0.00007652	0.005218
	Turbine Rotor Entry	0.000002134	0.02162
	Blade strike	0.0000006097	0.003683
	Collision and blade strike	0.0000003048	0.0001768
1.5 ms^{-1}	Zone of Influence	0.1240	0.3635
	Entrainment	0.08450	0.2833
	Collision	0.0002435	0.01466
	Turbine Rotor Entry	0.00003963	0.04374

	Blade strike	0.000006097	0.005966
	Collision and blade strike	0.0000009146	0.0003095
2.0 ms^{-1}	Zone of Influence	0.1199	0.3568
	Entrainment	0.08651	0.2897
	Collision	0.0004530	0.01873
	Turbine Rotor Entry	0.0001564	0.06054
	Blade strike	0.00001737	0.006986
	Collision and blade strike	0.0000009146	0.0004285
2.5 ms^{-1}	Zone of Influence	0.1205	0.3611
	Entrainment	0.08893	0.2991
	Collision	0.0008902	0.02255
	Turbine Rotor Entry	0.0004158	0.07145
	Blade strike	0.00003932	0.007864
	Collision and blade strike	0.000001829	0.0005476
3.0 ms^{-1}	Zone of Influence	0.1181	0.3592
	Entrainment	0.08930	0.3043
	Collision	0.001184	0.02501
	Turbine Rotor Entry	0.0007137	0.07081
	Blade strike	0.00007987	0.007766
	Collision and blade strike	0.000008231	0.0005749

3.3.4 *Sensitivity analysis*

A local sensitivity analysis indicates that entrainment is most sensitive model component to parameter value changes compared to all other model components. Entrainment has the greatest range of percent change estimates from the baseline mean, with axial-flow turbines being the most sensitive to parameter value changes (Table 8). Conversely, collision and blade strike probabilities are least sensitive compared to other volume-based model components due to less variability in probability estimates (Appendix A3.7, A3.8, A3.9). Percent change for collision from baseline parameter values arrange from -0.92 to -0.037%, and 0.0054 to 0.99% change for blade strike. For overall impacts, maximum turn angle is the most sensitive parameter influencing the probability of collision for an axial-flow turbine and blade strike for a cross-flow turbine. Avoidance strength

is the most sensitive parameter affecting the probability of collision for a cross-flow turbine (Table 8). Sequential collision and blade strike is omitted from the sensitivity analysis as no probabilities of impact were obtained.

Table 8. Percent changes of baseline mean values organized by model component, turbine type, and parameters from a 95% confidence interval for each 20% change. A dash in the columns indicate that a percent change was not quantified.

Model Component	Parameter	Percent Change	
		Δ 20%	Δ 20%
		Axial-Flow	Cross-Flow
Zone of Influence	Max turn angle	0.46	0.23
	Turn noise scale	0.11	0.12
	Avoidance strength	0.34	0.17
	Repulsion distance	0.45	0.21
	Attraction distance	1.44	0.11
	Alignment distance	1.27	0.16
	Desired direction weight	0.31	0.03
	Attraction & alignment weight	0.45	0.25
Entrainment	Max turn angle	5.04	1.29
	Turn noise scale	2.67	1.01
	Avoidance strength	9.40	7.64
	Repulsion distance	5.22	0.88

	Attraction distance	-1.82	-1.03
	Alignment distance	11.40	0.88
	Desired direction weight	7.13	2.60
	Attraction & alignment weight	-4.94	-0.11
Collision	Max turn angle	1.03	0.05
	Turn noise scale	—	0.068
	Avoidance strength	-0.97	0.15
	Repulsion distance	—	0.052
	Attraction distance	—	-0.037
	Alignment distance	—	0.056
	Desired direction weight	—	0.11
	Attraction & alignment weight	-0.92	-0.15
Blade strike	Max turn angle	—	0.99
	Turn noise scale	—	—
	Avoidance strength	—	0.0054
	Repulsion distance	—	—
	Attraction distance	—	—
	Alignment distance	—	—

Desired direction weight	—	—
Attraction & alignment weight	—	—

3.3.5 *Comparison of statistical model results to agent-based results*

Results from the statistical encounter-impact model are averaged based on model component and turbine type to enable comparison to average simulation encounter-impact results. Analyses from Wilcox t-tests (Wilcoxon, 1945) support evidence that the proportion of fish, adjusted for the number of fish in each model type, are different for each model component (Table 9). The greatest differences in average encounter-impact probabilities between the statistical and simulation models occur in the subcomponents of collision, blade strike, and sequential collision and blade strike. Simulation probabilities are one to four orders of magnitude lower than statistical probabilities. The remainder of model components are within the same order of magnitude across turbine type (Table 9).

Table 9. Comparison of average encounter-impact probabilities between the statistical and simulation-based model. Statistical probability estimates are based on day and night probabilities and avoidance. (*) indicate that averages from the statistical and simulation model are statistically significant.

Encounter-Impact Model Component	Average Statistical Encounter-Impact Probabilities	Average Simulation Encounter-Impact Probabilities	Average Statistical Encounter-Impact Probabilities	Average Simulation Encounter-Impact Probabilities
	Axial-Flow		Cross-Flow	

Zone of Influence	0.06425 *N = 4988*	0.02311* *N = 8856000* (12% of fish)	0.06425 *N = 4988*	0.08163* *N = 8856000* (37% of fish)
Entrainment	0.01820 *N = 129016*	0.001355* *N = 8856000* (7.5% of fish)	0.02221 *N = 22032*	0.01139* *N = 8856000* (26% of fish)
Collision	0.05430 *N = 48*	0.0003404* *N = 8856000*	0.05654 *N = 48*	0.01484* *N = 8856000*
Blade strike	0.06129 *N = 48*	0.00001422* *N = 8856000*	0.04984 *N = 48*	0.003779* *N = 8856000*
Collision and Blade strike	0.007458 *N = 48*	0.000001242* *N = 8856000*	0.007660 *N = 48*	0.0003562* *N = 8856000*

3.4 Discussion

Probability estimates of fish-turbine encounters and interactions, whether at individual or population levels, are influenced by the intricacies of model components, turbine designs, and experimental variables including fish abundance, aggregation behavior, and tidal flow. In the current model, tidal flow is the most important factor influencing fish-turbine interaction risk. At high tidal speeds, fish will drift into model components more frequently as tidal speed surpasses fish swimming speed. This results in fish potentially colliding with or being struck by turbine blades. Current encounter-impact models often do not include these behavioral or tidal flow conditions; therefore, it is important to include both active and passive avoidance behaviors when developing simulation encounter-impact models, especially since tidal turbine sites are located in high-flow environments (Pelc & Fujita, 2002).

Fish aggregation behavior also plays a fundamental role in how fish potentially encounter and/or interact with tidal turbines. Asocial fish exhibit lower probabilities of collision and/or blade strike compared to their socially-oriented counterparts. When schooling, fish prioritize aligning and fostering cohesion with neighboring individuals until individuals prioritize obstacle (i.e., turbine) avoidance over group formation and maneuvers (Domenici & Batty, 1997). This behavioral pattern is evident during low tidal speeds, where active swimming dictates fish trajectories, without any additional external environmental influences (Marras & Domenici, 2013). Results from the sensitivity analysis indicates that variation in aggregation parameters did not influence the impact component of the model. This suggests that chosen parameter values were robust and not merely artifacts of the model structure. In summary, tidal speed and social aggregation are two factors that heavily influence encounter-impact estimates. It is important to acknowledge that fish exhibit a wide range of behaviors beyond those simulated in the ABM, and

that hydrodynamics are more complex than the tidal flow and direction included in the model. Therefore, the association between tidal flow and aggregation, along with their respective encounter-impact probability estimates, are thought to represent maximum risks when applied to real-world scenarios.

Despite ABMs being a powerful tool that can incorporate empirical data and behavioral rule sets (c.f., Bonabeau, 2002), there are caveats to the interpretation of simulation results that should be addressed. ABMs can become computationally intensive as the number of agents and the complexity of interactions increase. For example, incorporating more complex behavioral and environmental conditions, such as fish predators, wind-induced waves, tides, or eddies, would require significantly more computational power or extended simulation run times. To maximize the efficiency of numerous simulation runs, we concentrated on the influence of social aggregation and tidal flow, to meet the objective of incorporating avoidance and aggregation behaviors in a fish-turbine interaction ABM.

In the context of this study, the lack of empirical data on aggregative and avoidance behaviors of individual fish poses a significant challenge when parameterizing an ABM. To mitigate this challenge, our study used aggregation parameters that mimicked fish movements from previous modeling studies by Couzin *et al.* (2002, 2005). By selecting parameters that represent herring behavior in our simulations, we found that parameter choices potentially influence encounter-impact probabilities. Results of the sensitivity analysis suggest that probabilities of impact were not artifacts of the model structure nor parameter choice. Impact probabilities exhibited minimal to no change from those estimated using baseline parameter values. Our model primarily focuses on simulating interactions up to collision and blade strike, we do not quantify direct injury, mortality, or any downstream indirect effects. Currently, such data

are unavailable, with the exception of Sanderson *et al.* (2023) who found no evidence of collisions or blade strikes when Atlantic salmon (*Salmo salar*) were examined downstream of a turbine installation. This data limitation restricts our ability to fully assess all impacts stemming from animal-device interactions. Our model also does not include other behaviors such as diel vertical migration (Rossington & Benson, 2020) that could enhance a fish's ability to evade a device at short or long approach distances. Incorporating more intricate behaviors into the simulation could potentially reduce probability estimates, as additional behavioral cues could increase device avoidance (c.f. Copping et al., 2021).

To date, few published marine and avian studies use simulation models to estimate interaction risks between animals and renewable energy devices. Eichhorn *et al.* (2012) developed an ABM to predict the risk of wind turbine blade and bird interactions based on bird proximity to wind turbines, integrating findings from the CRM (Band, 2006). They found that when 99-99.5% of birds recognize and actively avoid the wind turbine, the maximum annual mortality rate is 0.4 for birds within 1000 m of the device. In a MRE parallel example, Rossington and Benson (2020) developed a quasi-Lagrangian ABM to predict eel-turbine interactions to reproduce turbine rotor and interaction risk estimates from the CRM (Band et al., 2016). They used their ABM to integrate eel swimming speed, animal length, approach direction, and vertical migration scenarios, finding that 0.3-1.1% of eels will interact with the turbine. Variability in their probability estimates is largely dependent on eel swimming and vertical migration behaviors. Despite structural, focal species, and parameter value differences among the two published animal-turbine ABM models and this study, comparing numerical results from each simulation provides insight on how model parameters influence estimates of encounter-interaction risk. For example, Rossington & Benson's (2020) ABM estimated interaction risk to be two orders of magnitude higher than our axial-flow

turbine results, but their estimates are similar in order of magnitude to our cross-flow turbine results. This contrast suggests that differences in numerical outcomes may arise among turbine types, although these differences cannot be clearly separated from potential effects of including fish avoidance and aggregation behaviors in the current encounter-impact ABM.

A key insight gathered from our study is the comparison between results from the statistical model (q.v. Chapter 2.3) and the simulation model (q.v. Chapter 3.3). For the zone of influence and entrainment model components, spatial occupancy is within the same order of magnitude in both models, despite the Wilcox t-test (Wilcoxon, 1945) indicating that the means differ between the two sets of probabilities. In contrast, probabilities of overall impacts (i.e., collision, blade strike, collision and blade strike) differ by orders of magnitude among model and turbine types. For both turbine designs, overall impact statistical estimates are calculated using conditional probabilities of fish-turbine interactions and published literature values (e.g., Courtney et al., 2022; Romero-Gomez & Richmond, 2014; Yoshida et al., 2021) due to the lack of information on fish-turbine interactions in the Admiralty Inlet dataset. While overall impact simulation probabilities also incorporate literature-based probabilities, the simulation contains a tidal device with probabilities of turbine rotor passage or blade strike. Turbine rotor passage is an additional factor in the agent-based model, which results in lower overall blade strike and sequential collision and blade strike probabilities compared to the statistical model (c.f. Viehman & Zydlewski, 2015). The integration of spatial occupancy data and conditional probabilities from literature sources highlights significant differences in probability estimates of encounter and impact between the statistical and simulation models, emphasizing the importance of model selection in accurately assessing fish-turbine interaction risks.

A conceptual encounter-impact model was developed to serve as a framework for this and future modeling efforts using either a statistical or simulation approach. Potential improvements to the current simulation model could incorporate additional behaviors such as fish responses to light and turbine noise and expanding the model's scope to include more complex environmental characteristics (e.g., eddies, water levels, salinity) that may influence fish behaviors. Incorporating fish demographics and variations in schooling formations will increase the model's biological complexity but with a concurrent increase in realism. Integrating fully developed physical and hydrodynamic models (e.g., Salish Sea Model, Khangaonkar et al., 2017) within an ABM should further refine probability estimates of animal interactions with renewable energy devices. The simulation model can be further adapted to accommodate variable turbine rotor rotation with changes in tidal speed that will affect blade strike probabilities.

In summary, interactions between marine organisms and tidal turbines remain largely unquantified due to dynamic tidal sites limiting the efficacy of available optic and acoustic monitoring tools. As a complementary alternative, ABMs can be used to explore behavioral factors (e.g., aggregation and avoidance) that affect interactions between individuals, populations, and tidal turbines. This study provides insights into the dynamics of fish-turbine interactions, highlighting the influence of turbine design, fish abundance, aggregation behavior, and tidal speed on encounter and impact probabilities, which increases the understanding of factors impacting marine animal - MRE device interactions. Risk retirement is the process by which, based on current knowledge, risks associated with animals and MRE devices can be considered understood or effectively managed (Copping et al., 2020b). Regulators can use existing empirical data and encounter-impact models to accurately assess impact risks. This information can be then used to inform decisions related to turbine installation, operation, and mitigation regulations.

Chapter 4. Conclusions and Future Research

4.1 Review of the two modeling approaches

Statistical and simulation models each bring unique strengths and limitations to estimating probabilities of fish-turbine encounters and interactions. Statistical models rely on empirical data, while simulation models aim to replicate real-world processes over time, drawing conclusions from simulated system behaviors (Banks, 1999). The choice between these two models depends on research objectives, available data, and computational resources. Integrating insights from both approaches offers a consistency check of the results, a method to identify important data streams that may not yet exist, and the potential for comprehensive assessments of environmental impacts, especially in dynamic ecological systems such as tidal turbine sites.

4.1.1 *Fish positions and behaviors*

Animal behavior is complex and is challenging to replicate in modeling frameworks (Parrish & Edelstein-Keshet, 1999). Fish exhibit a wide range of behaviors, including intraspecies interactions, obstacle avoidance, locomotion, and aggregation (Lopez et al., 2012). Individual and aggregated fish trajectories are ideal for analyzing fish positions over time and can help predict whether fish are attracted to or will avoid structures such as tidal turbines.

In the statistical model, fish positions and avoidance behavior are inferred from the vertical spatial distribution data collected at Admiralty Inlet, WA, USA without additional assumptions. The accuracy of the model depends on the availability and quality of observational data, particularly individual animal trajectories, which are often limited by monitoring capabilities and data resolution (Williamson et al., 2017).

The simulation model simulates fish behaviors based on physiological constraints (e.g., swimming speed) and responses to environmental factors (e.g., tidal flow rates), which influence active and passive avoidance strategies. Simulation techniques can track individual fish trajectories in both space and time, enabling analysis of spatial distributions within model components or avoidance of turbines. However, simulations rely heavily on assumptions that must be validated with empirical data and those data streams may or may not be available. Regardless of the model structure, both the statistical and simulation model require sufficient data on complex animal positions and behaviors from the field to produce realistic results.

4.1.2 *Hydrodynamics*

Incorporating hydrodynamics into statistical or simulation modeling techniques adds complexity, often requiring the development or integration of specialized external models such as computational fluid dynamics or incorporating data from acoustic monitoring instruments like Acoustic Doppler Current Profilers (ADCPs). Both statistical and simulation models can use empirical data and hydrodynamic inputs to quantify flow fields at marine renewable energy (MRE) sites (e.g., Day et al., 2015), enabling evaluations of fish distributions and behaviors at flow velocities through tidal cycles. For example, our statistical model was parameterized with data obtained during both day and night, through a full tidal cycle. In the simulation model, we incorporated a range of tidal velocities to represent a full tidal cycle. The integration of hydrodynamics is crucial for analyzing interactions between animals and devices to provide insight on how these interactions vary with periodic environmental conditions.

4.1.3 *Computation*

Both model implementations involve trade-offs on assumptions, model structure, spatial-temporal resolution, and computational demands. The statistical model relies on available data and

reflects real-world conditions, but the efficacy is limited by sufficient and appropriate data streams. For example, the spatial limitation of the statistical model is evident in its inability to use two-dimensional data to estimate three-dimensional individual fish positions and avoidance behaviors. Although the Admiralty Inlet acoustic data were collected in three-dimensional space over time, the geometry of the echosounder beam (i.e., which represents a cone) causes the data to be reported as planar density. Using a multibeam sonar with a wide sampling swath up to 180 degrees could preserve the third dimension in spatial surveys.

The simulation model offers greater flexibility in spatial and temporal structuring, allowing simulations to be tailored to address specific research questions. The simulation model can also be used to calculate probabilities for populations of fish by incorporating social behaviors. This flexibility comes at the cost of increased computational complexity and resource demands. Simulation models are contingent on the rules and assumptions within the model, potentially introducing bias or inaccuracy that must be validated against empirical data. Additionally, changes in simulation run times, which may increase with model complexity, could present practical constraints depending on model application. In summary, the statistical model offers a foundational understanding of individual behaviors based on available data without relying on assumptions. In contrast, the simulation model allows for more flexibility in exploring complex interactions within populations, though introduces additional assumptions. Both models depend on the availability of data streams and computational resources, which must be considered when determining research objectives.

4.2 Future research

4.2.1 *Data availability*

Data availability is a crucial component that affects statistical and simulation model validation and accuracy. Both models developed in this study exemplify the use of empirical data from Admiralty Inlet where data from mobile echosounders, stationary ADCPs, and trawl catch surveys provide information on fish distribution species composition, and tidal velocity. In cases where the Admiralty Inlet data could not be used to parameterize specific model variables (e.g. collision and/or blade strike rates, herring aggregatory behaviors), both models used literature values as substitutes for missing parameter values. These parameter values are sourced from several MRE sites or laboratory settings, which could influence model accuracy and encounter-impact estimates.

To validate the encounter-impact probability model, a complete dataset of fish-turbine trajectories, encounters, and interactions are needed. Currently, there are only a few data streams available that are suitable for model use. Empirical data streams that are not currently available include fish colliding with stationary turbine structures (Müller et al., 2023; Peraza & Horne, 2023) and sequential collision and blade strike rates (Peraza & Horne, 2023). Blade strike rates from the field are also needed, as the few existing rates are derived from laboratory flume studies that do not accurately represent realistic tidal environments (e.g., Yoshida et al., 2020, 2021), or are captured in the field but during a short time period (i.e., 21 days) (e.g., Courtney et al., 2022). Capturing additional individual and aggregated fish trajectories from at least a hundred meters away from a turbine, similar to the data collected in Shen *et al.* (2016), will provide insights into fish behaviors related to active and passive avoidance and provide encounter data within the zone of influence and entrainment model components. Turbine noise is another factor to be considered

in data collection (Mitson, 1995), as hearing-sensitive fish, such as herring (Mitson, 2003), may detect low-frequency turbine noise from large distances (>100's m) that potentially serve as an initial cue for fish to avoid a device (Halvorsen et al., 2011). Once a robust dataset is obtained to validate the encounter-impact model, resource managers can potentially extend the use of the model to estimate mortality of a given species at a particular MRE site (Copping et al., 2023).

4.2.2 *Technology requirements for data acquisition*

There are different types of acoustic and optical technologies that can be used to acquire data appropriate for analyzing fish approach and interactions with MRE devices (c.f. Chapter 1). Mobile and stationary echosounders are effective tools for capturing fish trajectories as they approach tidal turbines (e.g., Shen et al., 2016). However, these technologies are unlikely to detect all fish across water depths, and often face challenges in classifying species within mixed fish communities (Williamson et al., 2017). Acoustic cameras can document interactions between fish and turbines (e.g., Bevelhimer et al., 2017; Viehman & Zydlewski, 2015), but any underwater optic instrument (e.g., DIDSON, Belcher et al., 2002) is limited in its detection range (Martignac et al., 2014), has image clarity dependent on water turbidity, and use artificial light to reduce these factors which can affect fish behavior around devices (Staines et al., 2022). Acoustic telemetry can also be used to monitor fish movement through space and time (e.g., Bangley et al., 2022; Sanderson et al., 2023) if hydrophone receivers and bathymetry provide complete coverage of a site. Acoustic telemetry systems can be deployed over several months, which can provide extensive monitoring of fish behavior near tidal devices. Through a combination of these technologies, a comprehensive dataset can be acquired to thoroughly investigate the behavior and interactions of fish around tidal turbine structures.

4.2.3 *Assessment of additional direct and delayed potential impacts*

Interactions between fish and tidal turbines can result in negative impacts, including collisions with turbine structures and blade strikes. These impacts exemplify direct interactions that may occur between animals and MRE devices. Barotrauma, resulting from sudden changes in pressure, can cause internal injuries to fish, particularly when exposed to rapid changes in water pressure near turbine blades (Brown et al., 2012). Shear stress refers to the force exerted on fish as water flow passes turbine blades, potentially causing physical damage or stress (Cada et al., 2007). Collecting data from tidal energy sites pose many challenges due to sites being high-energy environments with fast-moving and often turbid waters (Copping et al., 2020), making data collection difficult. For example, echoes of bubbles, drifting debris or solid surfaces such as rocks can result in poor quality data (Martignac et al., 2014). As an alternative, experimental flume studies (e.g., Amaral et al., 2015; Berry et al., 2019; Castro-Santos & Haro, 2015) have demonstrated potential fish-turbine effects and can be used to assess direct and delayed injury and/or mortality. Unfortunately, flume studies do not mimic real-world processes and the extent of injury or mortality from collisions and blade strikes remains uncertain.

Additional impacts of commercial-scale tidal arrays have not been evaluated. To maximize the economic benefits of capital infrastructure and power generation, an array of tidal turbines is necessary. Current research is largely focused on the effects of interactions with a single tidal turbine, but it remains unclear how these findings scale to large commercial sites and whether the presence and operation of multiple turbines introduce additional effects (Hasselman et al., 2024). These installations, which can occupy large areas of the seafloor, may alter fish migratory and foraging patterns, leading to further potential impacts (Hemery et al., 2021). Moving forward, it is crucial for future studies to expand beyond examining impacts of collision and blade strikes at the

scale of single turbines. Given the potential alterations to fish population displacement caused by large-scale commercial tidal arrays, comprehensive research is needed to assess additional impacts to ensure the sustainable deployment of tidal energy infrastructure.

4.3 Significance

The statistical and simulation implementations of the probabilistic encounter-impact model reveal several key insights. The statistical model found higher probabilities of encounter and impact at night with larger turbine structures, such as the representative cross-flow turbine used in this study. The simulation model highlights the importance of behavioral traits, such as avoidance influenced by fish active (i.e., swimming) or passive (i.e., drifting) locomotion and social aggregation, as crucial factors to prioritize in future models. Our series of tests on the three experimental factors in the simulation model demonstrate that tidal speed significantly affects fish-turbine interactions. Therefore, future modeling efforts should prioritize incorporating intricate fish behaviors and tidal speeds to ensure a comprehensive understanding of how these factors contribute to potential impacts from fish-turbine interactions or avoidance.

Additional research and empirical data collection are necessary to gain a thorough understanding of interactions between animals and MRE devices. While statistical and simulation models can help predict potential animal-turbine encounter and interaction rates, it is crucial to prioritize gathering data on how and when fish detect the turbine, and whether this triggers avoidance behavior at longer distances observed by Shen *et al.* (2016). Additional monitoring at tidal turbine structures can also reveal whether fish fail to avoid the turbine and hit the turbine base or are struck by its blades. These data can be used to quantify direct rates of injury or mortality. Information on potential injury or mortality rates from encounter-impact models are used by

regulators and managers when developing policies for tidal turbine deployment and operation in the U.S.

Concern over global climate change and reliance on the use of fossil fuels has increased interest in renewable energy technologies (Pelc & Fujita, 2002). The marine environment is an unexploited source of energy that could meet the global power demand (Inger et al., 2009). Nationally, the MRE industry seeks to produce renewable power through rivers and the ocean's waves, currents, and tides to meet energy needs. But before the industry can transition from demonstration projects to full-scale commercial sites, environmental impacts of operating turbines need to be quantified (Inger et al., 2009), which can be achieved through statistical and simulation modeling. The opportunity to introduce and invest research funds into marine renewable technologies will not only contribute to climate change mitigation strategies but can also provide economic and social benefits to coastal communities (Copping & Hemery, 2020). Economic and social impacts include providing a cleaner source of energy, local economic development, and the opportunity to create new jobs within the industry. Investment in MRE will grow employment and research opportunities at locations where there are high levels of wave energy (Pacific Ocean), tidal energy (Northeast, Pacific Northwest, and Alaskan coasts), ocean current energy (southern Atlantic coastline), and river current energy (LiVecchi et al., 2019).

Bibliography

Amaral, S., Bevelhimer, M., Čada, G., Giza, D., Jacobson, P., McMahon, B., & Pracheil, B. (2015). Evaluation of Behavior and Survival of Fish Exposed to an Axial-Flow Hydrokinetic Turbine. *North American Journal of Fisheries Management*, *35*, 97–113. https://doi.org/10.1080/02755947.2014.982333

An, L., Grimm, V., Sullivan, A., Turner II, B. L., Malleson, N., Heppenstall, A., Vincenot, C., Robinson, D., Ye, X., Liu, J., Lindkvist, E., & Tang, W. (2021). Challenges, tasks, and opportunities in modeling agent-based complex systems. *Ecological Modelling*, *457*, 109685. https://doi.org/10.1016/j.ecolmodel.2021.109685

Aoki, I. (1982). A simulation study on the schooling mechanism in fish. *NIPPON SUISAN GAKKAISHI*. https://doi.org/10.2331/suisan.48.1081

Band, B. (2012). Using a Collision Risk Model to Assess Bird Collision Risks for Offshore Wind Farms. Report by British Trust for Ornithology (BTO). Report for The Crown Estate.

Band B., Sparling C., Thompson D., Onoufriou J., San Martin E., West N. (2016). *Refining estimates of collision risk for harbour seals and tidal turbines: Scottish Marine and Freshwater Science Vol 7 No 17*. https://doi.org/10.7489/1786-1

Bangley, C. W., Hasselman, D. J., Flemming, J. M., Whoriskey, F. G., Culina, J., Enders, L., & Bradford, R. G. (2022). Modeling the Probability of Overlap Between Marine Fish Distributions and Marine Renewable Energy Infrastructure Using Acoustic Telemetry Data. *Frontiers in Marine Science*, *9*. https://www.frontiersin.org/articles/10.3389/fmars.2022.851757

Banks, J. (1999). Introduction to simulation. *Proceedings of the 31st Conference on Winter Simulation: Simulation---a Bridge to the Future - Volume 1*, 7–13. https://doi.org/10.1145/324138.324142

Belcher, E., Hanot, W., & Burch, J. (2002). Dual-Frequency Identification Sonar (DIDSON). *Proceedings of the 2002 Interntional Symposium on Underwater Technology (Cat. No.02EX556)*, 187–192. https://doi.org/10.1109/UT.2002.1002424

Bender, A., Langhamer, O., Francisco, F., Forslund, J., Hammar, L., Sundberg, J., & Molander, S. (2023). Imaging-sonar observations of salmonid interactions with a vertical axis instream turbine. *River Research and Applications*. https://doi.org/10.1002/rra.4171

Bernardi, S., & Scianna, M. (2020). An agent-based approach for modelling collective dynamics in animal groups distinguishing individual speed and orientation. *Philosophical*

Transactions of the Royal Society B: Biological Sciences, *375*(1807), 20190383. https://doi.org/10.1098/rstb.2019.0383

Berry M., Sundberg J., Francisco F. (2019). Salmonid response to a vertical axis hydrokinetic turbine in a stream aquarium. In 13th European Wave and Tidal Energy Conference (EWTEC).

Bevelhimer, M. S., Pracheil, B. M., Fortner, A. M., Saylor, R., & Deck, K. L. (2019). Mortality and injury assessment for three species of fish exposed to simulated turbine blade strike. *Canadian Journal of Fisheries and Aquatic Sciences*, *76*(12), 2350–2363. https://doi.org/10.1139/cjfas-2018-0386

Bevelhimer, M., Scherelis, C., Colby, J., & Adonizio, M. A. (2017). Hydroacoustic Assessment of Behavioral Responses by Fish Passing Near an Operating Tidal Turbine in the East River, New York. *Transactions of the American Fisheries Society*, *146*(5), 1028–1042. https://doi.org/10.1080/00028487.2017.1339637

Bonabeau, E. (2002). Agent-based modeling: Methods and techniques for simulating human systems. *Proceedings of the National Academy of Sciences*, *99*(suppl_3), 7280–7287. https://doi.org/10.1073/pnas.082080899

Brown, R. S., Carlson, T. J., Gingerich, A. J., Stephenson, J. R., Pflugrath, B. D., Welch, A. E., Langeslay, M. J., Ahmann, M. L., Johnson, R. L., Skalski, J. R., Seaburg, A. G., & Townsend, R. L. (2012). Quantifying Mortal Injury of Juvenile Chinook Salmon Exposed to Simulated Hydro-Turbine Passage. *Transactions of the American Fisheries Society*, *141*(1), 147–157. https://doi.org/10.1080/00028487.2011.650274

Buenau, K. E., Garavelli, L., Hemery, L. G., & García Medina, G. (2022). A Review of Modeling Approaches for Understanding and Monitoring the Environmental Effects of Marine Renewable Energy. *Journal of Marine Science and Engineering*, *10*(1), Article 1. https://doi.org/10.3390/jmse10010094

Cada, G., Ahlgrimm, J., Bahleda, M., Bigford, T., Stavrakas, S. D., Hall, D., Moursund, R., & Sale, M. (2007). Potential Impacts of Hydrokinetic and Wave Energy Conversion Technologies on Aquatic Environments. *Fisheries*, *32*(4), 174–181. https://doi.org/10.1577/1548-8446(2007)32[174:PIOHAW]2.0.CO;2

Castro-Santos, T., & Haro, A. (2015). Survival and Behavioral Effects of Exposure to a Hydrokinetic Turbine on Juvenile Atlantic Salmon and Adult American Shad. *Estuaries and Coasts*, *38*(1), 203–214. https://doi.org/10.1007/s12237-013-9680-6

Cavagnaro, R. J., Copping, A. E., Green, R., Greene, D., Jenne, S., Rose, D., & Overhus, D. (2020). Powering the Blue Economy: Progress Exploring Marine Renewable Energy Integration

With Ocean Observations. *Marine Technology Society Journal*, *54*(6), 114–125. https://doi.org/10.4031/MTSJ.54.6.11

Codling, E. A., Plank, M. J., & Benhamou, S. (2008). Random walk models in biology. *Journal of The Royal Society Interface*, *5*(25), 813–834. https://doi.org/10.1098/rsif.2008.0014

Copping, A. E., Freeman, M. C., Gorton, A. M., & Hemery, L. G. (2020b). Risk Retirement—Decreasing Uncertainty and Informing Consenting Processes for Marine Renewable Energy Development. *Journal of Marine Science and Engineering*, *8*(3), Article 3. https://doi.org/10.3390/jmse8030172

Copping, A. E., & Grear, M. E. (2018). Applying a simple model for estimating the likelihood of collision of marine mammals with tidal turbines. *International Marine Energy Journal*, *1*(1 (Aug)), Article 1 (Aug). https://doi.org/10.36688/imej.1.27-33

Copping, A. E., Hasselman, D. J., Bangley, C. W., Culina, J., & Carcas, M. (2023). A Probabilistic Methodology for Determining Collision Risk of Marine Animals with Tidal Energy Turbines. *Journal of Marine Science and Engineering*, *11*(11), Article 11. https://doi.org/10.3390/jmse11112151

Copping, A. E., Hemery, L. G., Viehman, H., Seitz, A. C., Staines, G. J., & Hasselman, D. J. (2021). Are fish in danger? A review of environmental effects of marine renewable energy on fishes. *Biological Conservation*, *262*, 109297. https://doi.org/10.1016/j.biocon.2021.109297

Copping, A., Grear, M., Jepsen, R., Chartrand, C., & Gorton, A. (2017). Understanding the potential risk to marine mammals from collision with tidal turbines. *International Journal of Marine Energy*, *19*, 110–123. https://doi.org/10.1016/j.ijome.2017.07.004

Copping, A., & Hemery, L. (2020). *OES-Environmental 2020 State of the Science Report* (PNNL--29976, 1632878; p. PNNL--29976, 1632878). https://doi.org/10.2172/1632878

Copping, A., Hemery, L., Overhus, D., Garavelli, L., Freeman, M., Whiting, J., Gorton, A., Farr, H., Rose, D., & Tugade, L. (2020a). Potential Environmental Effects of Marine Renewable Energy Development-The State of the Science. *Journal of Marine Science and Engineering*, *8*. https://doi.org/10.3390/jmse8110879

Courtney, M. B., Flanigan, A. J., Hostetter, M., & Seitz, A. C. (2022). Characterizing Sockeye Salmon Smolt Interactions with a Hydrokinetic Turbine in the Kvichak River, Alaska. *North American Journal of Fisheries Management*, *42*(4), 1054–1065. https://doi.org/10.1002/nafm.10806

Couzin, I. D., Krause, J., Franks, N. R., & Levin, S. A. (2005). Effective leadership and decision-making in animal groups on the move. *Nature*, *433*(7025), Article 7025. https://doi.org/10.1038/nature03236

Couzin, I. D., Krause, J., James, R., Ruxton, G. D., & Franks, N. R. (2002). Collective Memory and Spatial Sorting in Animal Groups. *Journal of Theoretical Biology*, *218*(1), 1–11. https://doi.org/10.1006/jtbi.2002.3065

Day, A. H., Babarit, A., Fontaine, A., He, Y.-P., Kraskowski, M., Murai, M., Penesis, I., Salvatore, F., & Shin, H.-K. (2015). Hydrodynamic modelling of marine renewable energy devices: A state of the art review. *Ocean Engineering*, *108*, 46–69. https://doi.org/10.1016/j.oceaneng.2015.05.036

DeAngelis, D. L., & Mooij, W. M. (2005). Individual-Based Modeling of Ecological and Evolutionary Processes. *Annual Review of Ecology, Evolution, and Systematics*, *36*, 147–168.

Domenici, P., & Batty, R. S. (1997). Escape behaviour of solitary herring (Clupea harengus) and comparisons with schooling individuals. *Marine Biology*, *128*(1), 29–38. https://doi.org/10.1007/s002270050065

Domenici, P., & Blake, R. W. (1997). The Kinematics and Performance of Fish Fast-Start Swimming. *Journal of Experimental Biology*, *200*(8), 1165–1178. https://doi.org/10.1242/jeb.200.8.1165

Eichhorn, M., Johst, K., Seppelt, R., & Drechsler, M. (2012). Model-Based Estimation of Collision Risks of Predatory Birds with Wind Turbines. *Ecology and Society*, *17*(2). https://doi.org/10.5751/ES-04594-170201

Fox, C. J., Benjamins, S., Masden, E. A., & Miller, R. (2018). Challenges and opportunities in monitoring the impacts of tidal-stream energy devices on marine vertebrates. *Renewable and Sustainable Energy Reviews*, *81*, 1926–1938. https://doi.org/10.1016/j.rser.2017.06.004

Frey, C. H., & Patil, S. R. (2002). Identification and Review of Sensitivity Analysis Methods. *Risk Analysis*, *22*(3), 553–578. https://doi.org/10.1111/0272-4332.00039

Gill, A. B. (2005). Offshore renewable energy: Ecological implications of generating electricity in the coastal zone. *Journal of Applied Ecology*, *42*(4), 605–615. https://doi.org/10.1111/j.1365-2664.2005.01060.x

Goodwin, R. A., Politano, M., Garvin, J. W., Nestler, J. M., Hay, D., Anderson, J. J., Weber, L. J., Dimperio, E., Smith, D. L., & Timko, M. (2014). Fish navigation of large dams emerges

from their modulation of flow field experience. *Proceedings of the National Academy of Sciences*, *111*(14), 5277–5282. https://doi.org/10.1073/pnas.1311874111

Goodwin, R. A., Smith, D. L., Nestler, J. M., Anderson, J. J., Weber, L. J., & Stockstill, R. L. (2012). *Agent-Based Approach Enhances Conventional Aquatic Habitat Description and Species Utilization Methods*. 1–8. https://doi.org/10.1061/40856(200)90

Grant M. C., Trinder M., Harding N. J. (2014). "A diving bird collision risk assessment framework for tidal turbines," in Scottish natural heritage commissioned report no. 773. Available at: https://tethys.pnnl.gov/sites/default/files/publications/SNH-2014.pdf.

Grippo, M., Zydlewski, G., Shen, H., & Goodwin, R. A. (2020). Behavioral responses of fish to a current-based hydrokinetic turbine under mutliple operational conditions. *Environmental Monitoring and Assessment*, *192*(10), 645. https://doi.org/10.1007/s10661-020-08596-5

Halvorsen, M., Carlson, T., & Copping, A. (2011). *Effects of Tidal Turbine Noise on Fish Task 2.1.3.2: Effects on Aquatic Organisms: Acoustics/Noise - Fiscal Year 2011 - Progress Report - Environmental Effects of Marine and Hydrokinetic Energy*.

Hammar, L., Andersson, S., Eggertsen, L., Haglund, J., Gullström, M., Ehnberg, J., & Molander, S. (2013). Hydrokinetic Turbine Effects on Fish Swimming Behaviour. *PLOS ONE*, *8*(12), e84141. https://doi.org/10.1371/journal.pone.0084141

Hammar, L., Eggertsen, L., Andersson, S., Ehnberg, J., Arvidsson, R., Gullström, M., & Molander, S. (2015). A Probabilistic Model for Hydrokinetic Turbine Collision Risks: Exploring Impacts on Fish. *PLOS ONE*, *10*(3), e0117756. https://doi.org/10.1371/journal.pone.0117756

Hasselman, D. J., Hemery, L. G., Copping, A. E., Fulton, E. A., Fox, J., Gill, A. B., & Polagye, B. (2023). 'Scaling up' our understanding of environmental effects of marine renewable energy development from single devices to large-scale commercial arrays. *Science of The Total Environment*, *904*, 166801. https://doi.org/10.1016/j.scitotenv.2023.166801

Hasselman, D. J., Hemery, L. G., Copping, A. E., Fulton, E. A., Gill, A. B., & Polagye, B. (2024). *Improving Understanding of Environmental Effects from Single MRE Devices to Arrays*.

He, P. (1993). Swimming speeds of marine fish in relation to fishing gears. *ICES Mar. Sci. Symp.*, *196*, 183–189.

Hemery, L. G., Copping, A. E., & Overhus, D. M. (2021). Biological Consequences of Marine Energy Development on Marine Animals. *Energies*, *14*(24), Article 24. https://doi.org/10.3390/en14248460

Horne J., Jacques D., Parker-Stetter S., Linder H., Nomura J. (2013). Evaluating Acoustic Technologies to Monitor Aquatic Organisms at Renewable Energy Sites Final Report (U.S. Dept. of the Interior, Bureau of Ocean Energy Management. BOEM), 2014–2057. Available at: https://espis.boem.gov/final%20reports/5415.pdf.

Huse, G., Railsback, S., & Feronö, A. (2002). Modelling changes in migration pattern of herring: Collective behaviour and numerical domination. *Journal of Fish Biology*, *60*(3), 571–582. https://doi.org/10.1111/j.1095-8649.2002.tb01685.x

Inger, R., Attrill, M. J., Bearhop, S., Broderick, A. C., James Grecian, W., Hodgson, D. J., Mills, C., Sheehan, E., Votier, S. C., Witt, M. J., & Godley, B. J. (2009). Marine renewable energy: Potential benefits to biodiversity? An urgent call for research. *Journal of Applied Ecology*, *46*(6), 1145–1153. https://doi.org/10.1111/j.1365-2664.2009.01697.x

Jacques, D. A. (2014). *Describing and Comparing Variability of Fish and Macrozooplankton Density at Marine Hydrokinetic Energy Sites* [Thesis]. https://digital.lib.washington.edu:443/researchworks/handle/1773/27479

Joy, R., Wood, J. D., Sparling, C. E., Tollit, D. J., Copping, A. E., & McConnell, B. J. (2018). Empirical measures of harbor seal behavior and avoidance of an operational tidal turbine. *Marine Pollution Bulletin*, *136*, 92–106. https://doi.org/10.1016/j.marpolbul.2018.08.052

Khangaonkar, T., Long, W., & Xu, W. (2017). Assessment of circulation and inter-basin transport in the Salish Sea including Johnstone Strait and Discovery Islands pathways. *Ocean Modelling*, *109*, 11–32. https://doi.org/10.1016/j.ocemod.2016.11.004

Li, H., Kolpas, A., Petzold, L., & Moehlis, J. (2009). Parallel simulation for a fish schooling model on a general-purpose graphics processing unit. *Concurrency and Computation: Practice and Experience*, *21*(6), 725–737. https://doi.org/10.1002/cpe.1330

LiVecchi, A., A. Copping, D. Jenne, A. Gorton, R. Preus, G. Gill, R. Robichaud, R. Green, S. Geerlofs, S. Gore, D. Hume, W. McShane, C. Schmaus, H. Spence. 2019. Powering the Blue Economy; Exploring Opportunities for Marine Renewable Energy in Maritime Markets. U.S. Department of Energy, Office of Energy Efficiency and Renewable Energy. Washington, D.C

Lopez, U., Gautrais, J., Couzin, I., & Theraulaz, G. (2012). *From behavioural analyses to models of collective motion in fish schools*. https://doi.org/10.1098/rsfs.2012.0033

Maclean, I. M. D., Inger, R., Benson, D., Booth, C. G., Embling, C. B., Grecian, W. J., Heymans, J. J., Plummer, K. E., Shackshaft, M., Sparling, C. E., Wilson, B., Wright, L. J., Bradbury, G., Christen, N., Godley, B. J., Jackson, A. C., McCluskie, A., Nicholls-Lee, R., & Bearhop, S. (2014). Resolving issues with environmental impact assessment of marine

renewable energy installations. *Frontiers in Marine Science*, *1*, 75. https://doi.org/10.3389/fmars.2014.00075

Marras, S., & Domenici, P. (2013). *Schooling Fish Under Attack Are Not All Equal: Some Lead, Others Follow | PLOS ONE*. doi:10.1371/ journal.pone.0065784

Martignac, F., Daroux, aurélie, Baglinière, J.-L., Ombredane, D., & Guillard, J. (2014). The use of acoustic cameras in shallow waters: New hydroacoustic tools for monitoring migratory fish population. A review of DIDSON technology. *Fish and Fisheries*. https://doi.org/10.1111/faf.12071

McLane, A. J., Semeniuk, C., McDermid, G. J., & Marceau, D. J. (2011). The role of agent-based models in wildlife ecology and management. *Ecological Modelling*, *222*(8), 1544–1556. https://doi.org/10.1016/j.ecolmodel.2011.01.020

Misund, O. A. (1993). Dynamics of moving masses: Variability in packing density, shape, and size among herring, sprat, and saithe schools. *ICES Journal of Marine Science*, *50*(2), 145–160. https://doi.org/10.1006/jmsc.1993.1016

Mitson, R. (2003). Causes and effects of underwater noise on fish abundance estimation. *Aquatic Living Resources*, *16*(3), 255–263. https://doi.org/10.1016/S0990-7440(03)00021-4

Mitson, R. B. (1995). *Underwater noise of research vessels: Review and recommendations* [Report]. ICES Cooperative Research Reports (CRR). https://doi.org/10.17895/ices.pub.5317

Muirhead, J., & Sprules, W. G. (2003). Reaction distance of Bythotrephes longimanus, encounter rate and index of prey risk for Harp Lake, Ontario. *Freshwater Biology*, *48*(1), 135–146. https://doi.org/10.1046/j.1365-2427.2003.00986.x

Müller, S., Muhawenimana, V., Sonnino-Sorisio, G., Wilson, C. A. M. E., Cable, J., & Ouro, P. (2023). Fish response to the presence of hydrokinetic turbines as a sustainable energy solution. *Scientific Reports*, *13*(1), Article 1. https://doi.org/10.1038/s41598-023-33000-w

Munk, P., Kiørboe, T., & Christensen, V. (1989). Vertical migrations of herring, Clupea harengus, larvae in relation to light and prey distribution. *Environmental Biology of Fishes*, *26*(2), 87–96. https://doi.org/10.1007/BF00001025

Murphy, K. J., Ciuti, S., & Kane, A. (2020). An introduction to agent-based models as an accessible surrogate to field-based research and teaching. *Ecology and Evolution*, *10*(22), 12482–12498. https://doi.org/10.1002/ece3.6848

Onoufriou, J., Brownlow, A., Moss, S., Hastie, G., & Thompson, D. (2019). Empirical determination of severe trauma in seals from collisions with tidal turbine blades. *Journal of Applied Ecology*, *56*(7), 1712–1724. https://doi.org/10.1111/1365-2664.13388

Parrish, J. K., & Edelstein-Keshet, L. (1999). Complexity, Pattern, and Evolutionary Trade-Offs in Animal Aggregation. *Science*, *284*(5411), 99–101. https://doi.org/10.1126/science.284.5411.99

Pelc, R., & Fujita, R. M. (2002). Renewable energy from the ocean. *Marine Policy*, *26*(6), 471–479. https://doi.org/10.1016/S0308-597X(02)00045-3

Peraza, J. I., & Horne, J. K. (2023). Quantifying conditional probabilities of fish-turbine encounters and impacts. *Frontiers in Marine Science*, *10*. https://www.frontiersin.org/articles/10.3389/fmars.2023.1270428

Polagye, B., Joslin, J., Murphy, P., Cotter, E., Scott, M., Gibbs, P., Bassett, C., & Stewart, A. (2020). Adaptable Monitoring Package Development and Deployment: Lessons Learned for Integrated Instrumentation at Marine Energy Sites. *Journal of Marine Science and Engineering*, *8*(8), Article 8. https://doi.org/10.3390/jmse8080553

Reynolds, C. W. (1987). Flocks, herds and schools: A distributed behavioral model. *ACM SIGGRAPH Computer Graphics*, *21*(4), 25–34. https://doi.org/10.1145/37402.37406

Roche, R. C., Walker-Springett, K., Robins, P. E., Jones, J., Veneruso, G., Whitton, T. A., Piano, M., Ward, S. L., Duce, C. E., Waggitt, J. J., Walker-Springett, G. R., Neill, S. P., Lewis, M. J., & King, J. W. (2016). Research priorities for assessing potential impacts of emerging marine renewable energy technologies: Insights from developments in Wales (UK). *Renewable Energy*, *99*, 1327–1341. https://doi.org/10.1016/j.renene.2016.08.035

Romero-Gomez, P., & Richmond, M. C. (2014). Simulating blade-strike on fish passing through marine hydrokinetic turbines. *Renewable Energy*, *71*, 401–413. https://doi.org/10.1016/j.renene.2014.05.051

Rose, D., Freeman, M., & Copping, A. (2023). Engaging the Regulatory Community to Aid Environmental Consenting/Permitting Processes for Marine Renewable Energy. *International Marine Energy Journal*, *6*(2), 55–61. https://doi.org/10.36688/imej.6.55-61

Rose, K. A., Rutherford, E. S., McDermot, D. S., Forney, J. L., & Mills, E. L. (1999). Individual-Based Model of Yellow Perch and Walleye Populations in Oneida Lake. *Ecological Monographs*, *69*(2), 127–154. https://doi.org/10.1890/0012-9615(1999)069[0127:IBMOYP]2.0.CO;2

Rossington, K., & Benson, T. (2020). An agent-based model to predict fish collisions with tidal stream turbines. *Renewable Energy*, *151*, 1220–1229. https://doi.org/10.1016/j.renene.2019.11.127

Saltelli, A. (Ed.). (2004). *Sensitivity analysis in practice: A guide to assessing scientific models*. Wiley.

Saltelli, A. (Ed.). (2008). *Global sensitivity analysis: The primer*. Wiley.

Sanderson, B. G., Bangley, C. W., McGarry, L. P., & Hasselman, D. J. (2023). Measuring Detection Efficiency of High-Residency Acoustic Signals for Estimating Probability of Fish–Turbine Encounter in a Fast-Flowing Tidal Passage. *Journal of Marine Science and Engineering*, *11*(6), Article 6. https://doi.org/10.3390/jmse11061172

Sanderson, B. G., Karsten, R. H., Solda, C. C., Hardie, D. C., & Hasselman, D. J. (2023). Probability of Atlantic Salmon Post-Smolts Encountering a Tidal Turbine Installation in Minas Passage, Bay of Fundy. *Journal of Marine Science and Engineering*, *11*(5), Article 5. https://doi.org/10.3390/jmse11051095

Schmitt, P., Culloch, R., Lieber, L., Molander, S., Hammar, L., & Kregting, L. (2017). A tool for simulating collision probabilities of animals with marine renewable energy devices. *PLOS ONE*, *12*(11), e0188780. https://doi.org/10.1371/journal.pone.0188780

Shen, H., Zydlewski, G. B., Viehman, H. A., & Staines, G. (2016). Estimating the probability of fish encountering a marine hydrokinetic device. *Renewable Energy*, *97*, 746–756. https://doi.org/10.1016/j.renene.2016.06.026

Shields, M. A., Woolf, D. K., Grist, E. P. M., Kerr, S. A., Jackson, A. C., Harris, R. E., Bell, M. C., Beharie, R., Want, A., Osalusi, E., Gibb, S. W., & Side, J. (2011). Marine renewable energy: The ecological implications of altering the hydrodynamics of the marine environment. *Ocean & Coastal Management*, *54*(1), 2–9. https://doi.org/10.1016/j.ocecoaman.2010.10.036

Simmonds, J., & MacLennan, D. (Eds.). (2005). *Fisheries Acoustics: Theory and Practice* (1st ed.). Wiley. https://doi.org/10.1002/9780470995303

Staines, G. J., Mueller, R. P., Seitz, A. C., Evans, M. D., O'Byrne, P. W., & Wosnik, M. (2022). Capabilities of an Acoustic Camera to Inform Fish Collision Risk with Current Energy Converter Turbines. *Journal of Marine Science and Engineering*, *10*(4), Article 4. https://doi.org/10.3390/jmse10040483

Staines, G., Zydlewski, G. B., Viehman, H. A., & Kocik, R. (2020). Applying Two Active Acoustic Technologies to Document Presence of Large Marine Animal Targets at a Marine

Renewable Energy Site. *Journal of Marine Science and Engineering*, *8*(9), Article 9. https://doi.org/10.3390/jmse8090704

Thomas, G. L., Kirsch, J., & Thorne, R. E. (2002). Ex Situ Target Strength Measurements of Pacific Herring and Pacific Sand Lance. *North American Journal of Fisheries Management*, *22*(4), 1136–1145. https://doi.org/10.1577/1548-8675(2002)022<1136:ESTSMO>2.0.CO;2

Utne, A. C. W. (1997). The effect of turbidity and illumination on the reaction distance and search time of the marine planktivore Gobiusculus flavescens. *Journal of Fish Biology*, *50*(5), 926–938. https://doi.org/10.1111/j.1095-8649.1997.tb01619.x

Viehman, H. A., & Zydlewski, G. B. (2015). Fish Interactions with a Commercial-Scale Tidal Energy Device in the Natural Environment. *Estuaries and Coasts*, *38*(1), 241–252. https://doi.org/10.1007/s12237-014-9767-8

Viehman, H. A., Zydlewski, G. B., McCleave, J. D., & Staines, G. J. (2015). Using Hydroacoustics to Understand Fish Presence and Vertical Distribution in a Tidally Dynamic Region Targeted for Energy Extraction. *Estuaries and Coasts*, *38*(1), 215–226. https://doi.org/10.1007/s12237-014-9776-7

Wilcoxon, F. (1945). Individual Comparisons by Ranking Methods. *Biometrics Bulletin*, *1*(6), 80–83. https://doi.org/10.2307/3001968

Williamson, B., Fraser, S., Williamson, L., Nikora, V., & Scott, B. (2019). Predictable changes in fish school characteristics due to a tidal turbine support structure. *Renewable Energy*, *141*, 1092–1102. https://doi.org/10.1016/j.renene.2019.04.065

Williamson, B. J., Blondel, P., Armstrong, E., Bell, P. S., Hall, C., Waggitt, J. J., & Scott, B. E. (2016). A Self-Contained Subsea Platform for Acoustic Monitoring of the Environment Around Marine Renewable Energy Devices–Field Deployments at Wave and Tidal Energy Sites in Orkney, Scotland. *IEEE Journal of Oceanic Engineering*, *41*(1), 67–81. https://doi.org/10.1109/JOE.2015.2410851

Williamson, B. J., Fraser, S., Blondel, P., Bell, P. S., Waggitt, J. J., & Scott, B. E. (2017). Multisensor Acoustic Tracking of Fish and Seabird Behavior Around Tidal Turbine Structures in Scotland. *IEEE Journal of Oceanic Engineering*, *42*(4), 948–965. https://doi.org/10.1109/JOE.2016.2637179

Wilson, B., Batty, R., Daunt, F., & Carter, C. (2006). *Collision risks between marine renewable energy devices and mammals, fish and diving birds. Report to the Scottish Executive*.

Yoshida, T., Furuichi, D., Williamson, B. J., Zhou, J., Dong, S., Li, Q., & Kitazawa, D. (2021). Experimental study of fish behavior near a tidal turbine model under dark conditions. *Journal of Marine Science and Technology*. https://doi.org/10.1007/s00773-021-00850-w

Yoshida, T., Zhou, J., Park, S., Muto, H., & Kitazawa, D. (2020). Use of a model turbine to investigate the high striking risk of fish with tidal and oceanic current turbine blades under slow rotational speed. *Sustainable Energy Technologies and Assessments*, *37*, 100634. https://doi.org/10.1016/j.seta.2020.100634

Zhang, J., Kitazawa, D., Taya, S., & Mizukami, Y. (2017). Impact assessment of marine current turbines on fish behavior using an experimental approach based on the similarity law. *Journal of Marine Science and Technology*, *22*(2), 219–230. https://doi.org/10.1007/s00773-016-0405-y

Appendix A2

Appendix A2.1: Model component estimates for an axial-flow turbine during day.

Model Component				Active Avoidance		Passive Avoidance	
Domain	1						
Zone of Influence	0.0636						
Entrainment							
Empirical	0.00245						
Admiralty Inlet avoidance	0.0118			0.0236		0.790	
Shen *et al.* (2016) avoidance	0.0399			0.372		0	
Collision	Courtney *et al.* 2022	Yoshida *et al*. 2021	Romero-Gomez and Richmond, 2014	Zone of Influence (Shen *et al*. 2016)	Entrainment (Viehman and Zydlewski, 2015)	Zone of Influence (Shen *et al.* 2016)	Entrainment (Viehman and Zydlewski, 2015)
No avoidance	0.0374	0.0408	0.0258 - 0.0372		0.020		0.937
Admiralty Inlet avoidance	0.000443	0.000484	0.000305 - 0.000441	0.0236	0.020	0.790	0.937

Shen *et al.* (2016) avoidance	0.00149	0.00163	0.000103 - 0.00148	0.372	0.020	0	0.937
Blade strike							
Literature	0.13	0.05	0.40 - 0.133				
Admiralty Inlet avoidance	0.00154	0.000592	0.00473 - 0.00157	0.0236		0.790	
Shen *et al.* (2016) avoidance	0.00519	0.00199	0.0159 - 0.00532	0.372		0	
Collision and blade strike							
No avoidance	0.00486	0.00204	0.0103 - 0.00496		0.020		0.937
Admiralty Inlet avoidance	0.0000576	0.0000242	0.000122 - 0.0000588	0.0236	0.020	0.790	0.937
Shen *et al.* (2016) avoidance	0.000194	0.0000815	0.000412 - 0.000198	0.372	0.020	0	0.937

Appendix A2.2: Model component estimates for an axial-flow turbine at night.

Model Component				Active Avoidance		Passive Avoidance	
Domain	1						
Zone of Influence	0.0649						
Entrainment							
Empirical	0.00250						
Admiralty Inlet avoidance	0.0118			0.0241		0.792	
Shen *et al.* (2016) avoidance	0.0408			0.372		0	
Collision	Courtney *et al*. 2022	Yoshida *et al.* 2021	Romero-Gomez and Richmond, 2014	Zone of Influence (Shen *et al.* 2016)	Entrainment (Viehman and Zydlewski, 2015)	Zone of Influence (Shen *et al.* 2016)	Entrainment (Viehman and Zydlewski, 2015)
No avoidance	0.288	0.324	0.199 - 0.287		0.109		0.559
Admiralty Inlet avoidance	0.00343	0.00385	0.00236 - 0.00342	0.0241	0.109	0.790	0.559
Shen *et al.* (2016) avoidance	0.0117	0.0132	0.00812 - 0.0117	0.372	0.109	0	0.559
Blade strike							

Literature	0.13	0.022	0.40 - 0.133				
Admiralty Inlet avoidance	0.00154	0.000261	0.00475 - 0.00158	0.0241		0.792	
Shen *et al.* (2016) avoidance	0.00530	0.000987	0.0163 - 0.00544	0.372		0	
Collision and blade strike							
No avoidance	0.0375	0.00714	0.0678 - 0.0347		0.109		0.559
Admiralty Inlet avoidance	0.000446	0.0000849	0.000947 - 0.000456	0.0241	0.109	0.792	0.559
Shen *et al.* (2016) avoidance	0.00153	0.000291	0.00325 - 0.00156	0.372	0.109	0	0.559

Appendix A2.3: Model component estimates for a cross-flow turbine during day.

Model Component				Active Avoidance		Passive Avoidance	
Domain	1						
Zone of Influence	0.0636						
Entrainment							
Empirical	0.0144						
Admiralty Inlet avoidance	0.0118			0.0236		0.790	
Shen *et al.* (2016) avoidance	0.0399			0.372		0	
Collision	Courtney *et al.* 2022	Yoshida *et al.* 2021	Romero-Gomez and Richmond, 2014	Zone of Influence (Shen *et al.* 2016)	Entrainment (Viehman and Zydlewski, 2015)	Zone of Influence (Shen *et al.* 2016)	Entrainment (Viehman and Zydlewski, 2015)
No avoidance	0.0374	0.0408	0.0307 - 0.0389		0.020		0.937
Admiralty Inlet avoidance	0.000443	0.000484	0.000364 - 0.000461	0.0236	0.020	0.790	0.937
Shen *et al.* (2016) avoidance	0.00149	0.00163	0.00122 - 0.00155	0.372	0.020	0	0.937
Blade strike							

Literature	0.13	0.05	0.285 - 0.0951				
Admiralty Inlet avoidance	0.00154	0.000592	0.00845 - 0.00140	0.0236		0.790	
Shen *et al.* (2016) avoidance	0.00519	0.00199	0.0284 - 0.00474	0.372		0	
Collision and blade strike							
No avoidance	0.00486	0.00204	0.0219 -0.00462		0.020		0.937
Admiralty Inlet avoidance	0.0000576	0.0000242	0.000259 - 0.0000548	0.0236	0.020	0.790	0.937
Shen *et al.* (2016) avoidance	0.000194	0.0000815	0.000875 - 0.000184	0.372	0.020	0	0.937

Appendix A2.4: Model component estimates for a cross-flow turbine at night.

Model Component				Active Avoidance		Passive Avoidance	
Domain	1						
Zone of Influence	0.0649						
Entrainment							
Empirical	0.0146						
Admiralty Inlet avoidance	0.0118			0.0241		0.792	
Shen *et al.* (2016) avoidance	0.0408			0.372		0	
Collision	Courtney *et al.* 2022	Yoshida *et al.* 2021	Romero-Gomez and Richmond, 2014	Zone of Influence (Shen *et al.* 2016)	Entrainment (Viehman and Zydlewski, 2015)	Zone of Influence (Shen *et al.* 2016)	Entrainment (Viehman and Zydlewski, 2015)
No avoidance	0.288	0.324	0.237 - 0.300		0.109		0.559
Admiralty Inlet avoidance	0.00343	0.00385	0.00113 - 0.00347	0.0241	0.109	0.790	0.559
Shen *et al.* (2016) avoidance	0.0117	0.0132	0.00388 - 0.0119	0.372	0.109	0	0.559
Blade strike							

Literature	0.13	0.022	0.285 - 0.0951				
Admiralty Inlet avoidance	0.00154	0.000261	0.00847 - 0.00141	0.0241		0.792	
Shen *et al.* (2016) avoidance	0.00530	0.000897	0.0291 - 0.00485	0.372		0	
Collision and blade strike							
No avoidance	0.0375	0.00714	0.0678 - 0.0285		0.109		0.559
Admiralty Inlet avoidance	0.000446	0.0000849	0.000806 - 0.000413	0.0241	0.109	0.792	0.559
Shen *et al.* (2016) avoidance	0.00153	0.000291	0.00277 - 0.00141	0.372	0.109	0	0.559

Appendix A3

Appendix A3.1. Individual fish trajectory probabilities for the zone of influence organized by turbine type (i.e., axial-flow, cross-flow), fish abundance (i.e., 164, 328, 656), and tidal speed (ms^{-1}). Probabilities are on the y-axis for each corresponding boxplot with ranges exhibiting zero to maximum probabilities per model component. Tidal speed is organized on the x-axis from 0 to 3.0 ms-1. Fish behavior is organized into three categories of aggregation behavior (i.e., asocial, semi-social, social).

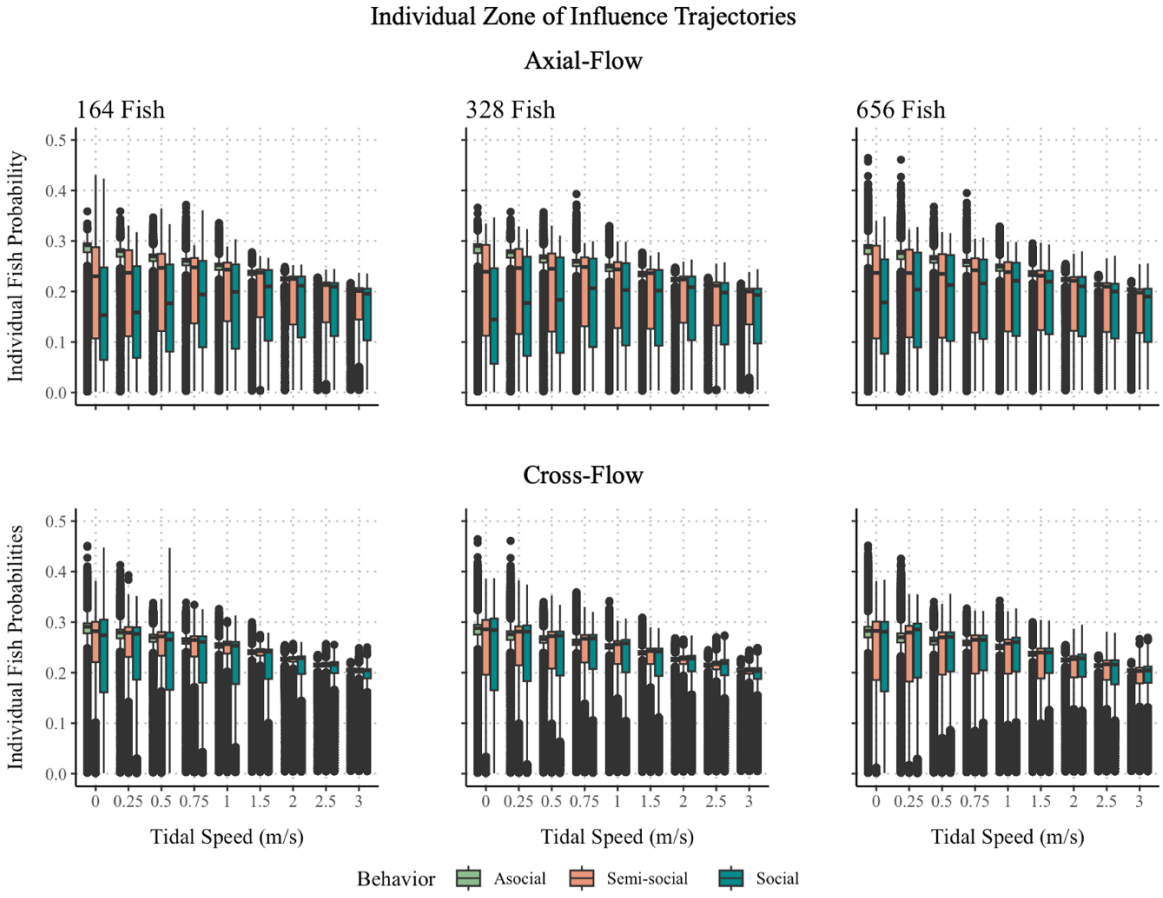

Appendix A3.2. Population probabilities for the zone of influence organized by turbine type (i.e., axial-flow, cross-flow), fish abundance (i.e., 164, 328, 656), and tidal speed (ms^{-1}). Tidal speed is organized on the x-axis from 0 to 3.0 ms-1. Fish behavior is organized into three categories of aggregation behavior (i.e., asocial, semi-social, social).

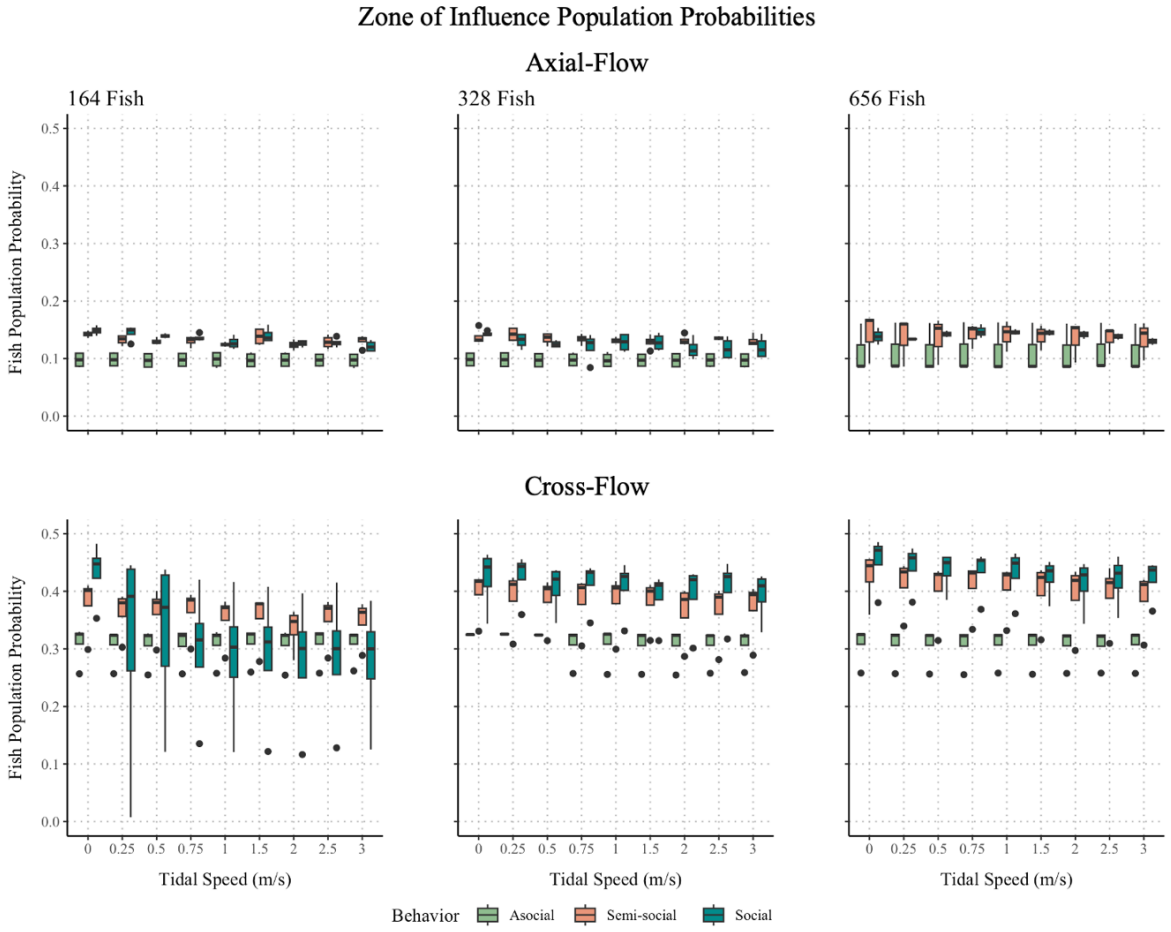

Appendix A3.3. Individual fish trajectory probabilities for the entrainment component organized by turbine type (i.e., axial-flow, cross-flow), fish abundance (i.e., 164, 328, 656), and tidal speed (ms^{-1}). Probabilities are on the y-axis for each corresponding boxplot with ranges exhibiting zero to maximum probabilities per model component. Tidal speed is organized on the x-axis from 0 to 3.0 ms-1. Fish behavior is organized into three categories of aggregation behavior (i.e., asocial, semi-social, social).

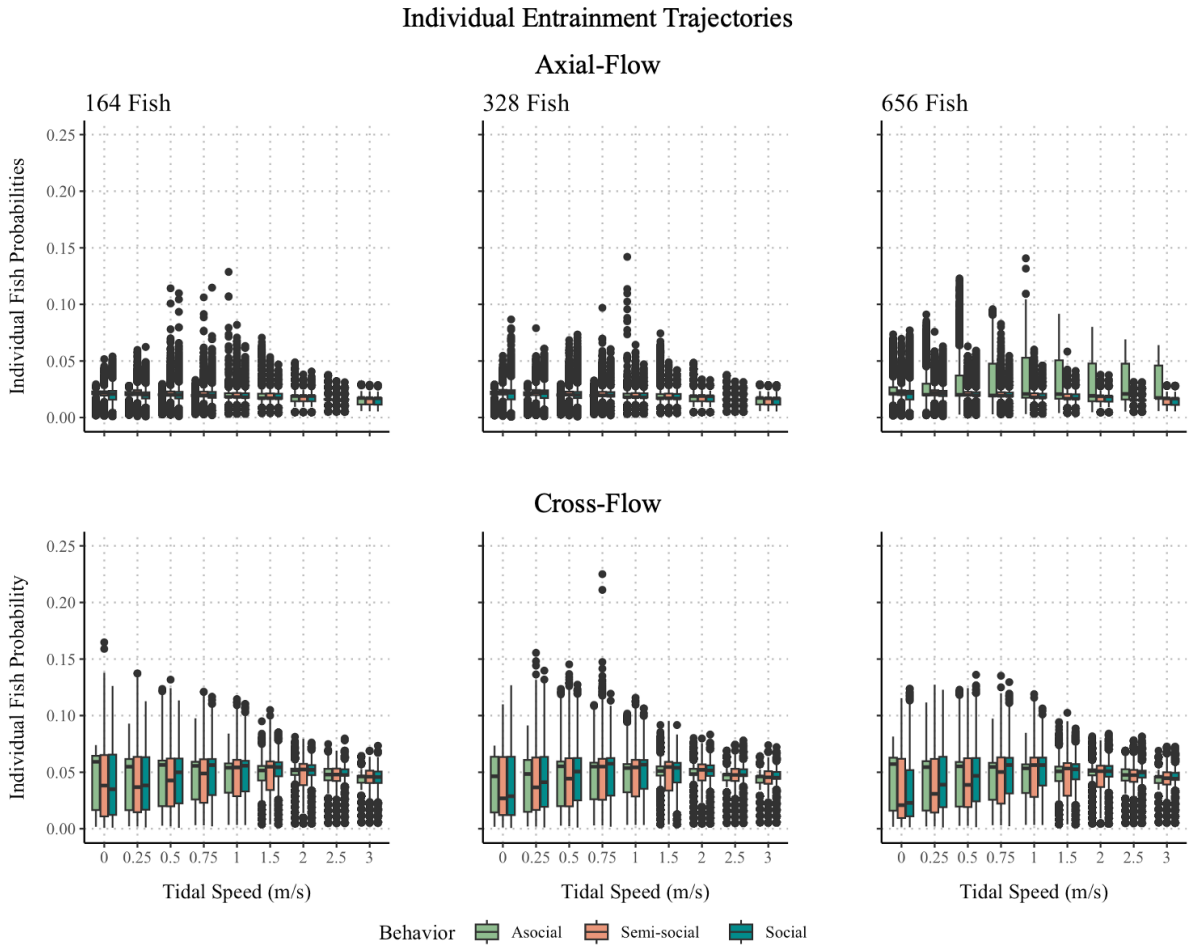

Appendix A3.4. Population probabilities for the entrainment component organized by turbine type (i.e., axial-flow, cross-flow), fish abundance (i.e., 164, 328, 656), and tidal speed (ms^{-1}). Tidal speed is organized on the x-axis from 0 to 3.0 ms-1. Fish behavior is organized into three categories of aggregation behavior (i.e., asocial, semi-social, social).

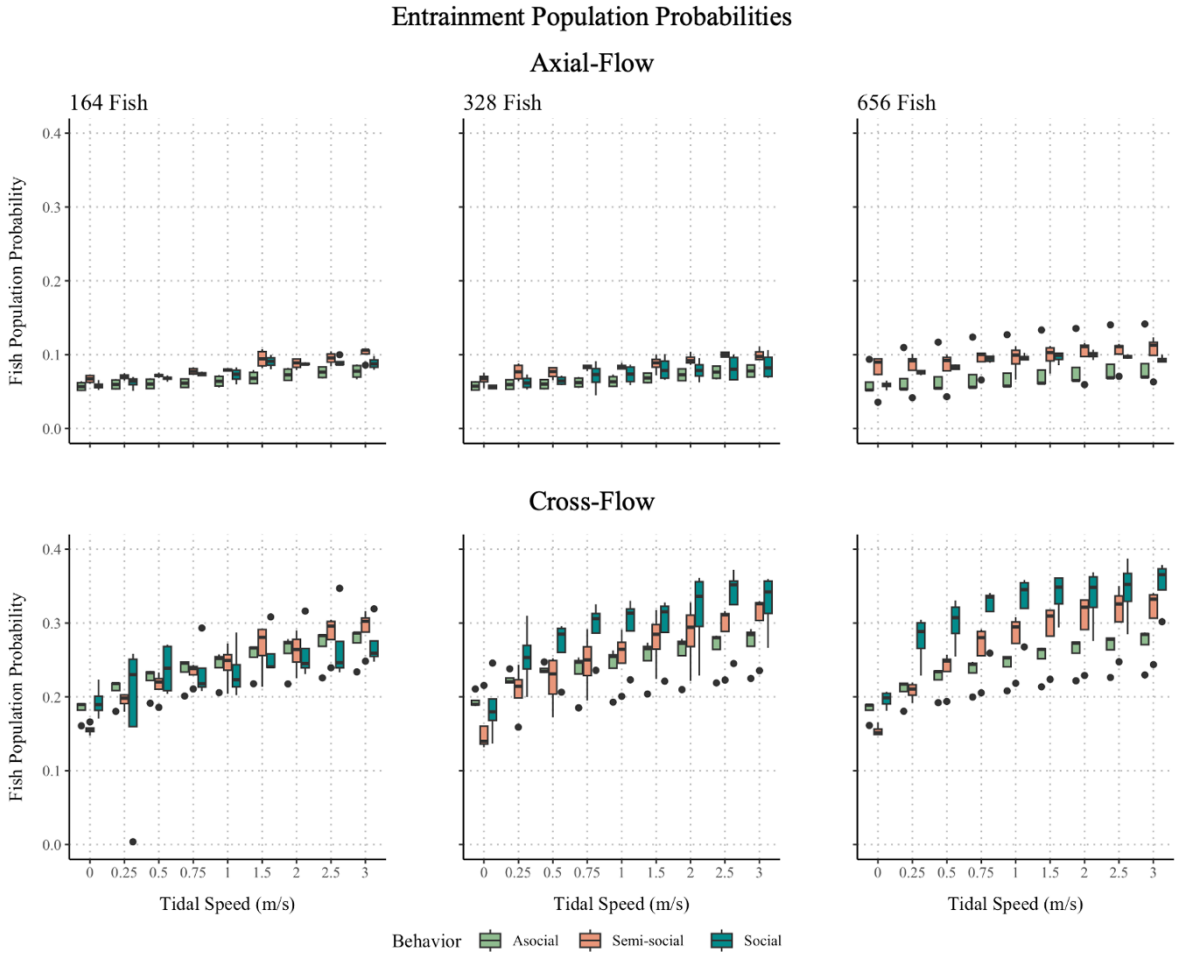

Appendix A3.5. Individual fish trajectory probabilities for the turbine rotor-swept area organized by turbine type (i.e., axial-flow, cross-flow), fish abundance (i.e., 164, 328, 656), and tidal speed (ms^{-1}). Probabilities are on the y-axis for each corresponding boxplot with ranges exhibiting zero to maximum probabilities per model component. Tidal speed is organized on the x-axis from 0 to 3.0 ms-1. Fish behavior is organized into three categories of aggregation behavior (i.e., asocial, semi-social, social).

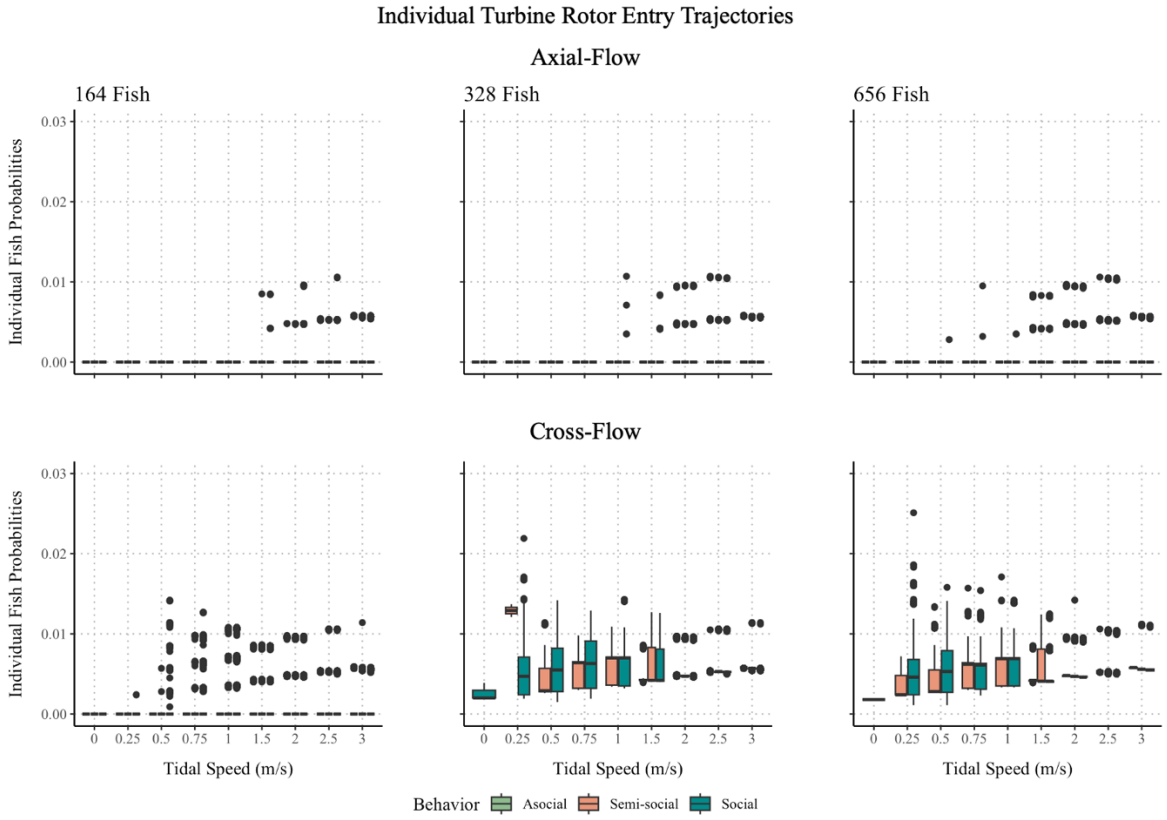

Appendix A3.6. Population probabilities for the turbine rotor-swept area organized by turbine type (i.e., axial-flow, cross-flow), fish abundance (i.e., 164, 328, 656), and tidal speed (ms^{-1}). Tidal speed is organized on the x-axis from 0 to 3.0 ms-1. Fish behavior is organized into three categories of aggregation behavior (i.e., asocial, semi-social, social).

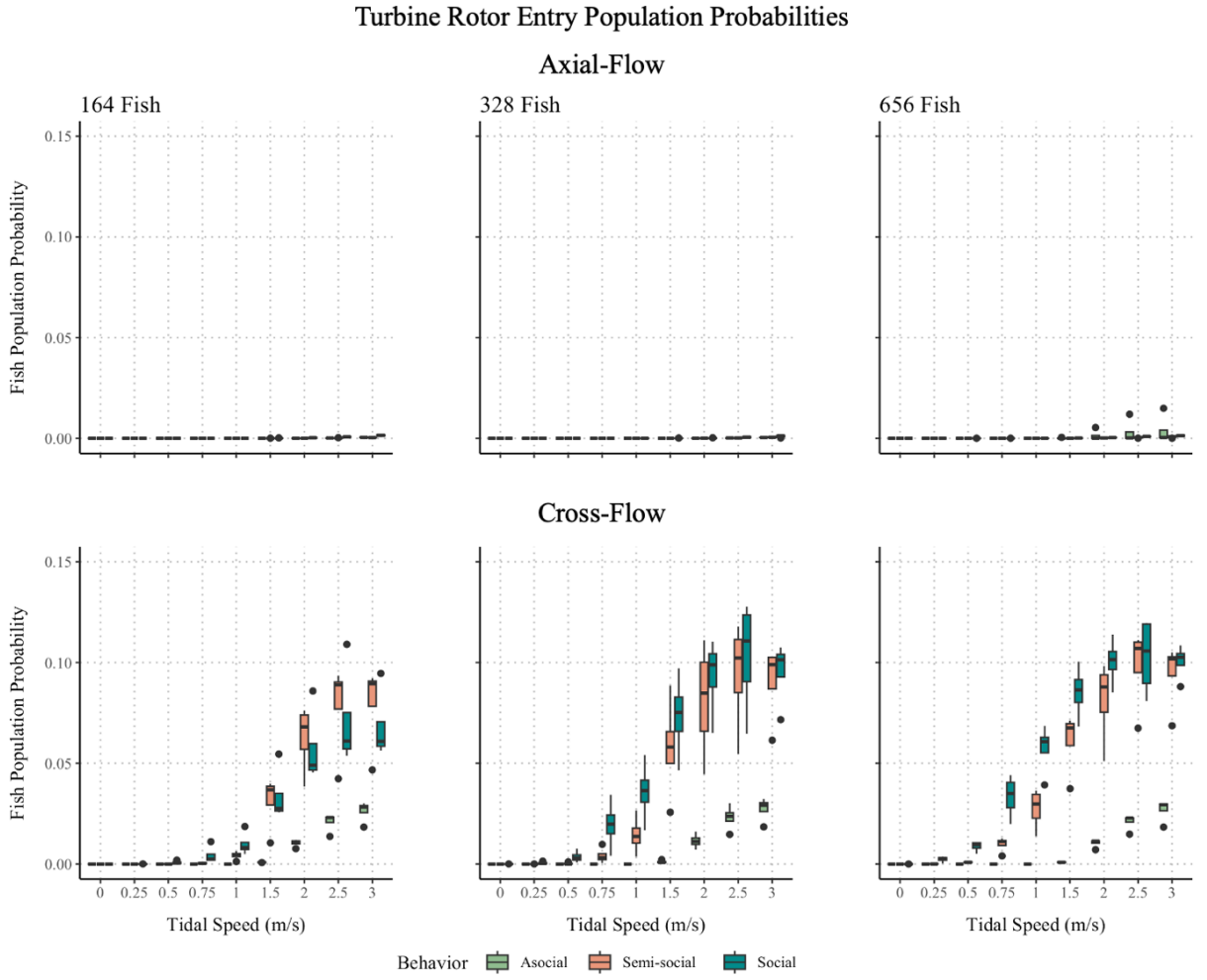

Appendix A3.7. Population probabilities for collision are organized by turbine type (i.e., axial-flow, cross-flow), fish abundance (i.e., 164, 328, 656), and tidal speed (ms^{-1}). Tidal speed is organized on the x-axis from 0 to 3.0 ms-1. Fish behavior is organized into three categories of aggregation behavior (i.e., asocial, semi-social, social).

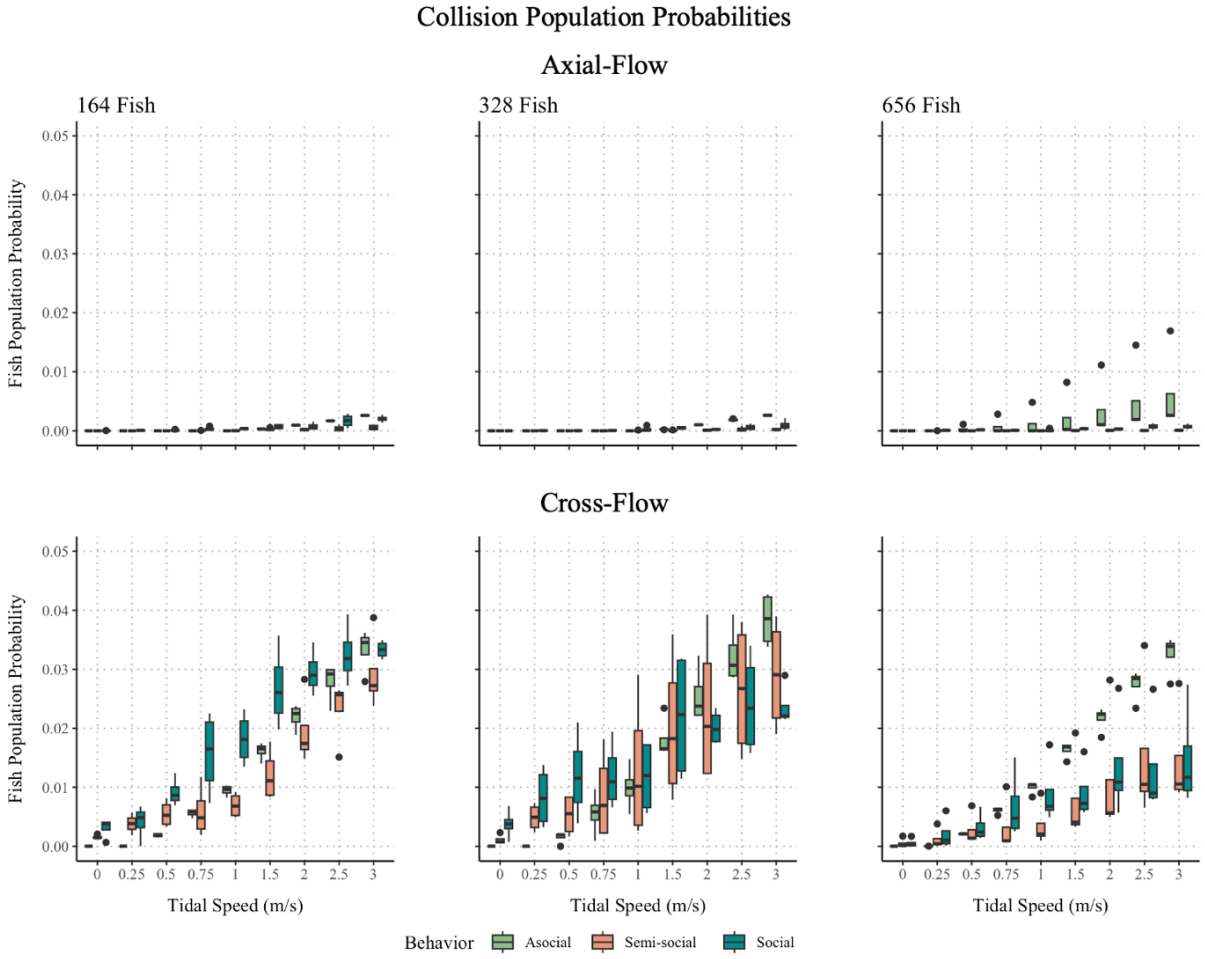

Appendix A3.8. Population probabilities for blade strike are organized by turbine type (i.e., axial-flow, cross-flow), fish abundance (i.e., 164, 328, 656), and tidal speed (ms^{-1}). Tidal speed is organized on the x-axis from 0 to 3.0 ms-1. Fish behavior is organized into three categories of aggregation behavior (i.e., asocial, semi-social, social).

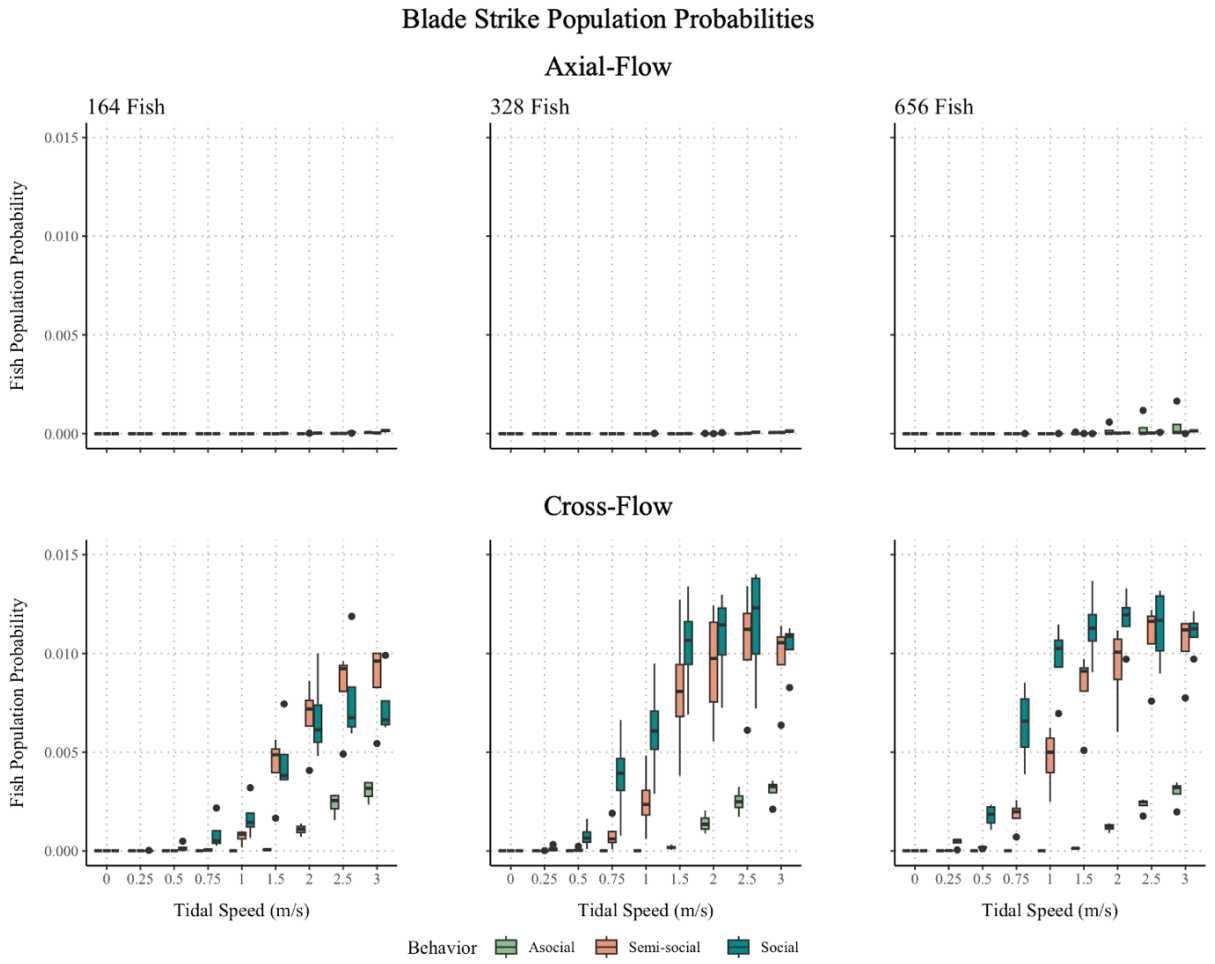

Appendix A3.9. Population probabilities for sequential collision and blade strike are organized by turbine type (i.e., axial-flow, cross-flow), fish abundance (i.e., 164, 328, 656), and tidal speed (ms^{-1}). Tidal speed is organized on the x-axis from 0 to 3.0 ms-1. Fish behavior is organized into three categories of aggregation behavior (i.e., asocial, semi-social, social).